The BMP antagonist CHORDIN as a regulator of osteoclast formation and function: an in vitro study

By

Hesam Abbas-Tehrani

A thesis submitted in partial fulfillment of the requirements for the degree of

Master of Science

Medical Sciences-Periodontology

University of Alberta

Abstract

Periodontitis is a multifactorial chronic inflammatory disease of the periodontium characterized by clinical attachment loss, alveolar bone loss, deep probing depths, and gingivitis. In susceptible individuals, the shift from gingivitis to periodontitis represents a stage which the bacterial challenge has overwhelmed the immune system and any tissue repair is unlikely. Although there is a wealth of knowledge regarding the microbiology of periodontitis, there is still a lack of understanding with respect to the factors that govern the transition from gingivitis to periodontitis.

Alveolar bone loss is the hallmark of periodontal disease which is mediated by osteoclasts. The signalling networks that in addition to the RANKL/RANK/OPG network regulate the differentiation of osteoclasts are poorly understood.

Bone morphogenic proteins (BMPs) are growth factors with a diverse function affecting many tissues throughout the body such as the formation of bone, tooth, cartilage, and many more. In recent years the effect of BMPs on bone resorption has gained considerable attention. Studies show that the same BMPs that induced bone formation via osteoblasts are also responsible for bone resorption via osteoclasts.

In support of this, Graf et al. have shown that BMP2 and its antagonists Twisted Gastrulation (TWSG1) and Chordin (CHRD) were expressed at site of alveolar bone resorption in a periodontal injury model. Therefore, we speculate that the expression of BMP2 and its antagonists in close vicinity to resorption sites may affect osteoclast differentiation and function.

In this project, we have taken in-vitro approaches to determine how CHRD regulates osteoclastogenesis. We identified that BMP2, CHRD, and TWSG1 are all induced in early differentiating osteoclasts. Osteoclast differentiation from bone marrow cells did not seem to be altered in CHRD-deficient mice.

The characterization of the in-vitro role of CHRD on BMP signaling during osteoclastogenesis is significant, as it reinforces the importance of BMP signalling network in bone remodelling. These new results also help to refine our current understanding of the various effects of recombinant BMP2 in alveolar bone regeneration.

Preface

This thesis is the original work of Hesam Abbas-Tehrani. Our research project, received research ethics approval from the University of Alberta's Research Ethics Board entitled "The BMP antagonist CHORDIN as a regulator of osteoclast formation and function: an in-vitro study.": No AUP1149

As the author my role involved preforming literature review, study design, data collection, data analysis and performing experiments.

Dedication

I want to dedicate this thesis to my mother and father, to whom I owe all my accomplishments and successes in my life. I am forever grateful for their support and sacrifice.

بنام خداوند خورشید و ماه که دل را بنامش خرد داد راه

خداوند هستی و هم راستی نخواهد ز تو کژی و کاستی

اگر بوسیدن دست عیب و عار است درباره من همین کار برای مادر و پدرم افتخار است

اگر هر چه هستم یا هر که هستم از نعمت وجود نازنین و گرانقدر آنهاست

آنان که برای من از جان مایه گذاشتند بیشتر از جان خود دوستشان دارم

زبان از توصیفشان عاجز و قلم از شرح خوبیها یشان ناتوان است

پایان نامه تخصص خود را که نتیجه ایثار و فداکاری آنان است با احترام و تعظیم به حضورشان تقدیم میدارم

Acknowledgments

During the past three years, my thesis project evolved through many failures and successes. Dr. Graf has provided me with support, encouragement and knowledge throughout my research project, and I would like to thank him for giving me the opportunity to work in his lab. Over the past three years, I developed invaluable problem-solving skills and learnt the importance of perseverance which I will take forward with me as I begin my career.

I would like to thank my supervisory committee, Drs. Ava Chow and Douglas Dederich for their valuable feedback about my thesis during my committee meetings.

I am forever grateful to have had Dr. Maria Alexiou teach me the fundamentals, protocols and procedures related to my research project. Dr. Alexiou has been a great mentor, providing me with continuous support and motivation.

I am indebted to Farah Eaton and Pranidhi Baddam for their help in the various aspects of my research project. I would also like to thank all the students in Dr. Graf's lab for their assistance.

Finally, I want to thank my best friend Ghazaleh for all her support and helping with the editorial aspects of this thesis.

Table of Contents

List of Tables

Chapter 1:

Chapter 3:

Chapter 4:

List of Figures

Chapter 1:

Chapter 4:

Abbreviations

36B4- House-keeping gene

ATP6V0d2- ATPase, H+ transporting, lysosomal 38 kDa, V0 subunit d2

BMP- Bone Morphogenetic Protein

BV- Bone Volume

c-Fms- Colony Stimulating Factor Receptor 1

c-fos- fos transcription factor

CF- Circular Fibers

CHRD- Chordin

CTR- Calcitonin Receptor

CTSK- Cathepsin K

DC-STAMP- Dendritic Cell Specific Transmembrane Protein

DGF- Dento-Gingival Fibers

DPF- Dento-Periosteal Fibers

FGF- Fibroblast Growth Factor

GRM1- Gremlin1

IGF- Insulin-like Growth Factor

IL- Interleukins

LPs- Lipopolysaccharide

M-CSF- Macrophage Colony Stimulating Factor

MMP- Matrix Metalloproteinases

NFATc1- Nuclear Factor of Activated T-cells, cytoplasmic 1

OC-STAMP- Osteoclast Specific Transmembrane Protein

OPG- Osteoprotegrin

Osx- Osterix

PDGF- Platelet-Derived Growth Factor

PDL- Periodontal Ligament

PGE2- Prostaglandin E2

PMN- Polymorphonuclear Neutrophils

RANK- Receptor Activator of Nuclear factor-Kappa beta

RANKL- RANK ligand

RUNX2- Runt-Related Transcription Factor 2

Tb. Th- Trabecular Thickness

Tb.Sp- Trabecular Spacing

TCR- T-cell Receptor

TF- Transeptal Fibers

TGF- Transforming Growth Factor

TGFβ- Transforming Growth Factor beta

TNF-α- Tumor Necrosis Factor α

TRAP- Tartrate-Resistant Acid Phosphatase

TV- Total Volume

TWSG1- Twisted Gastrulation

VEGF- Vascular Endothelial Growth Factor

β3- Integrin β3

Chapter 1: Introduction

Chapter 1.1: Anatomy of the Periodontium

The human dentition is maintained and supported by a complex called the periodontium. The periodontium is composed four components: gingiva, root cementum, periodontal ligament, and alveolar bone proper (Fig. 1). Each of these components have distinct locations and vary in their histological and architectural composition. However, they are all connected as a functional unit to attach the teeth to the bones of the jaws, maintain the integrity of the surface mucosa of the oral cavity, protect the dentition against invading pathogens, and receptors to transmit nociception and proprioception.

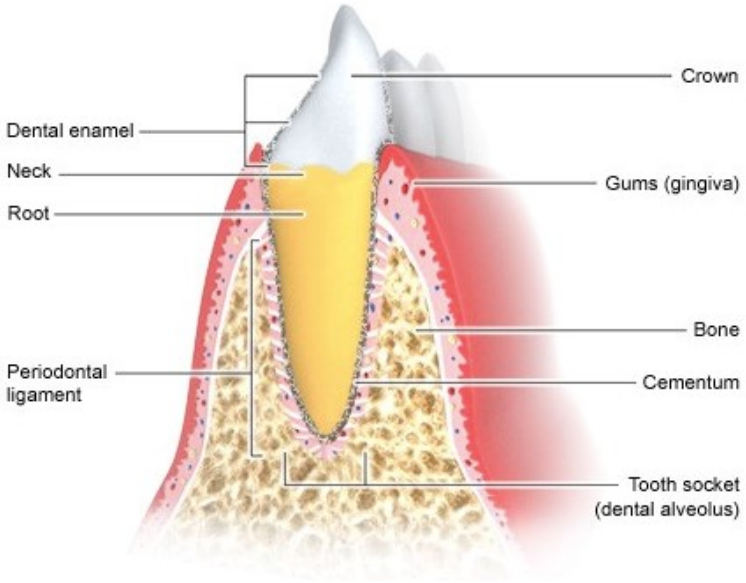

Figure 1: Schematic cross-section through the tooth complex. Structures of the periodontium include the gingiva, cementum, periodontal ligament, alveolar bone.

1.1.1) Gingiva

The oral mucosa is continuous with the skin of the lips and extends posteriorly to include the mucosa of the soft palate and pharynx. Within this boundary the oral mucosa in divided into three distinct zones (Fig. 2):

1) Masticatory mucosa: includes tissues covering the hard palate and gingiva
2) Specialized mucosa: covering the dorsum surface of the tongue
3) Lining mucosa (alveolar mucosa): covering the remainder of the oral cavity.

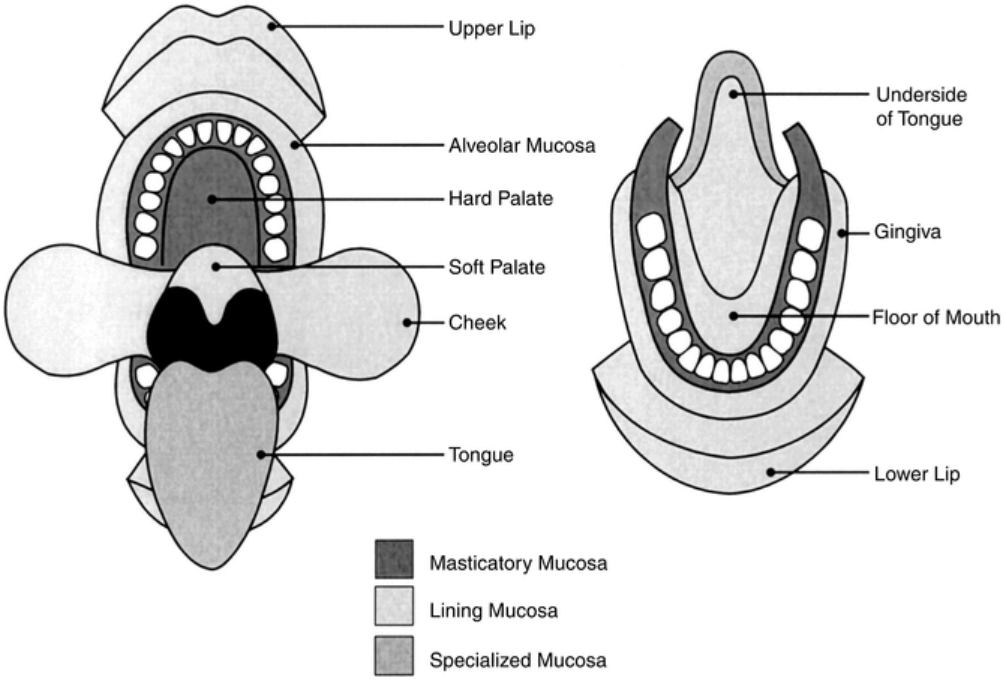

Figure 2: Schematic showing the different zones of the oral mucosa. Adopted from https://www.slideshare.net/jeansara85/oral-mucous-membrane-10313924

In a healthy adult, the gingiva covers the alveolar bone and extends to cover the tooth to a level slightly coronal to the cementoenamel junction.

Macroscopically, the gingiva is divided into three parts: marginal, attached, and interdental gingival tissues (Fig. 3). There is considerable variation amongst the three areas in terms of differentiation, histology and thickness, however, all function to resist mechanical and microbial damage.

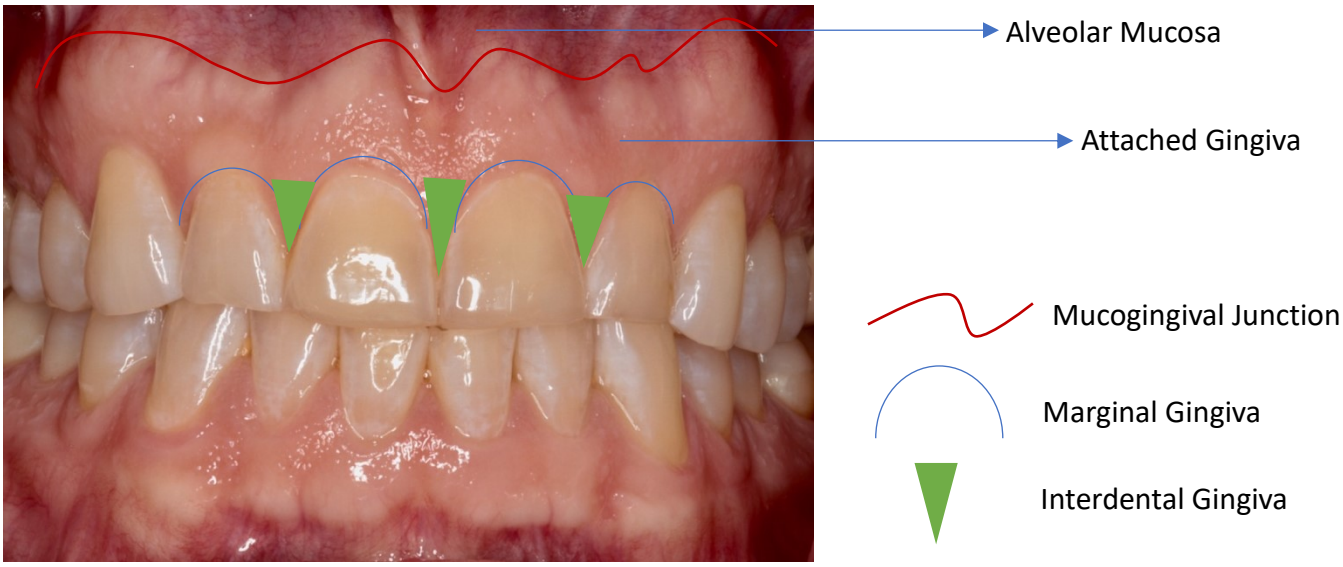

Figure 3: Frontal intra-oral picture showing the 3 zones of the gingiva. The mucogingival line represents the demarcation line between the alveolar mucosa and attached gingiva.

On a microscopic level, the gingiva is divided into an outer stratified squamous epithelium layer and an underlying connective tissue layer.

The connective tissue layer is mostly composed of collagen fibers arranged in bundles that have variable orientation. These fibers are termed gingival fibers and are categorized according to their insertion and path in the tissue. These include circular fibers, dento-gingival fibers, dento-periosteal fibers, and transeptal fibers (Fig. 4). These fibers function to firmly attach the marginal

gingiva to the tooth and root cementum, provide rigidity to withstand masticatory forces and a physical barrier to microbial challenges.

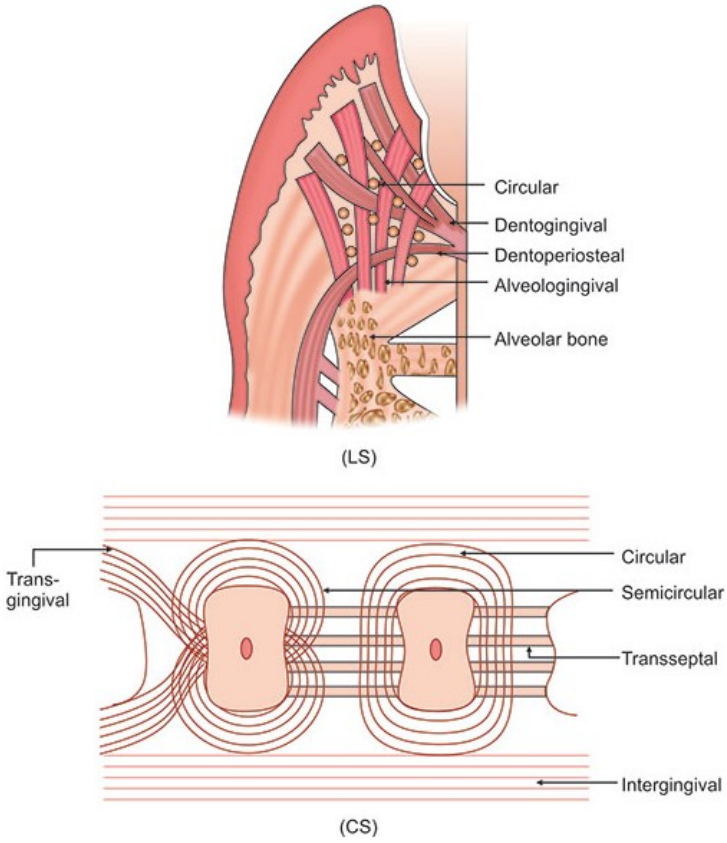

Figure 4: Schematic showing the different gingival fibers present in the connective tissue layer of the gingiva.

Aside from providing a mechanical or physical barrier to infection, the epithelium has the necessary arsenal to neutralize various pathogens. The gingival tissues are capable of recruiting neutrophils, macrophages and lymphocytes to the site of microbial invasion. In doing so, these immune cells form a wall against the pathogens in order to destroy them and prevent their progression to the underlying tissues of the periodontium[1]. In susceptible individuals, these protective mechanisms are breached exposing the underlying tissues and cells to the pathogenic

components. Consequently, virulence factor from the pathogens stimulates cellular components including monocytes and fibroblasts to produce many pro-inflammatory cytokines (IL-1, IL-6, IL-8, TNF-α, PGE2, MMPs). These cytokines act alone or in concert resulting in alveolar bone resorption via osteoclasts, connective tissue and periodontal ligament destruction via MMPs[1].

1.1.2) Periodontal Ligament

The periodontal ligament (PDL) space, on average 0.2mm wide, encompasses a complex vasculature, lymphatic system and a highly cellular connective tissue[2]. The predominant component of the periodontal ligament is made up of collagen called principal fibers. These fibers surround the entire tooth root at one end and connect into the alveolar bone at opposite end. The terminal insertion into the root cementum and alveolar bone are called Sharpey's fibers. Like the gingival fiber, the principal fibers are arranged into bundles and have a variable course in the periodontal ligament space. They are categorized according to their orientation and/or location. These include the alveolar crest, oblique, horizontal, apical, and interradicular fibers[3] (Fig. 5).

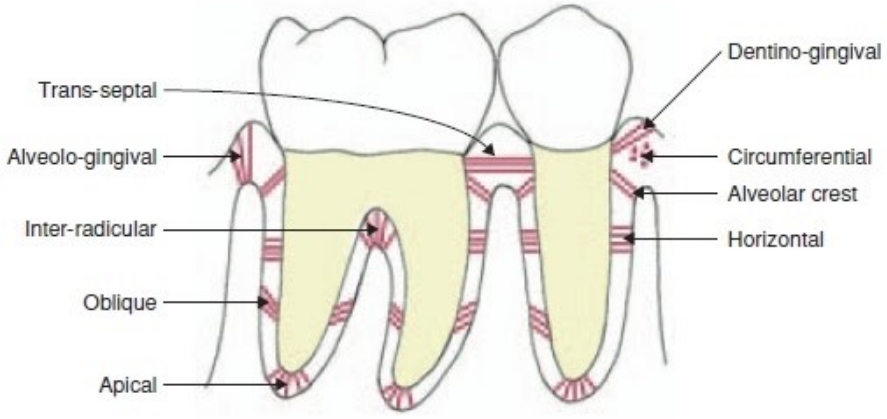

Figure 5: Schematic showing the different principal periodontal ligament space. These fibers connect the root to the alveolar bone.

The principal fibers together with the cellular, vascular, lymphatic, and nervous system of the periodontal ligament provide a variety of functions which are categorized as physical, formative and remodelling, and nutritional and sensory functions[3].

Physical function: the periodontal ligament protects the vessels and nerves from injury due to mechanical forces. The principal fibers act as shock absorbers to reduce the occlusal forces and transmit these forces to the alveolar bone.

Formative and remodeling: the periodontal ligament and alveolar bone are constantly being exposed to physical forces such as masticatory, parafunctional, and orthodontic forces[4]. In response to these forces, progenitor cells in the PDL differentiate into mature osteoblasts and osteoclasts. An example is the "pressure-tension" theory in orthodontic tooth movement which states that when PDL fibers sense mechanical queues osteoclasts at the compression side resorb bone while osteoblasts at the tension side secrete new bone matrix[1].

Nutritional and sensory: the vasculature present in the periodontal ligament provides nutrients to the root cementum, alveolar bone, and gingival tissues. There is also a lymphatic system which removes waste and toxins from these same tissues. The neural pathways closely accompany the vasculature and are located along the mid-root area and extend to the apical region. They can transmit proprioception, pressure, and pain sensation via the trigeminal nervous system[5].

1.1.3) Root Cementum

The root surface is covered by cementum which is a mineralized tissue. The inorganic component, mainly hydroxyapatite crystals accounts for 65% of weight while collagen fibrils contribute the most to the organic component[1]. It is an avascular tissue that has no lymph or innervations. Cementum does not go through homeostatic remodeling rather it is characterized by continuous deposition throughout life. This phenomenon better allows the tooth to over erupt in order to compensate for attrition. The cementum attaches the principal fibers of the periodontal ligament to the root surface and participates in the repair of the root surface if damaged.

The cementum can experience resorption due to a variety of local, systemic, or idiopathic factors. These resorptions can be microscopic in nature or extensive enough to be detected on radiographs. In most cases, the resorption is not continuous and may be interrupted with periods of deposition of new cementum. The newly formed cementum is demarcated by a reversal line which depicts the border of the resorption area[3].

Cementoblasts are needed to regenerate cementum. This is crucial for maintaining the periodontium during development and regenerating lost periodontal tissues. Research has shown that the epithelial cells rests of Malassez may be involved in cementum repair and regeneration[6]. Their activation secrets matrix proteins such as amelogenins, enamelins, and others which are expressed during tooth development. In addition, studies have shown the potential role of several growth factors involved in cementum regeneration. These include the transforming growth factor family (bone morphogenic proteins), enamel matrix derivatives, platelet derived growth factors, and insulin growth factors[7].

1.1.4) Alveolar Bone Proper

The alveolar process is part of the maxilla and mandible which forms and supports the bony socket around the roots of teeth. It is composed of about 67% inorganic matrix by weight. Calcium and potassium are main components of the inorganic matter with the mineral content found primarily in the form of calcium hydroxyapatite crystals. The remaining 33% is made up of organic material[1]. The main component of the organic matrix is collagen; however, non-collagenous material is also present.

The alveolar process is divided into three areas which include[3]:

1) Cortical bone: forms the external part and consist of a compact network of bone lamellae.
2) Alveolar bone proper: makes up the inner surface of the socket wall and consists of a thin compact bone. It contains many openings through which the neurovascular bundles from the periodontal ligament communicate with the cancellous bone.
3) Cancellous bone: bone trabeculation with irregular shaped marrow spaces which exist and supports the external and internal compact bone.

The development of the alveolar process is dependent on tooth formation and eruption. Hence, once a tooth is removed or lost there is a gradual resorption of the alveolar process. It is for these reasons that the shape, size, location, and function of teeth dictates the morphology of the alveolar process.

As mentioned previously, the tooth is anchored firmly in their sockets by means of principal fibers which develop from the root cementum and extend into the alveolar process. The main function of alveolar process is to absorb and distribute masticatory, parafunctional, orthodontic forces.

The cells present in the alveolar bone include osteocytes, osteoblasts, and osteoclasts which are responsible for the remodeling of the alveolar bone in response to different physiological forces and pathogenic microorganisms. In addition, a number of local and systemic factors influences the remodelling process which ultimately affects the height, contour, and density of the alveolar process.

In summary, the periodontium can be viewed as having distinct components, all of which function together to maintain the integrity and protect the tooth complex. Whether there is an insult from pathogens and/or mechanical stresses the periodontal tissues respond by inducing complex molecular pathways with a net result of either bone remodeling or just bone resorption with the goal of adapting to a new environment. Although there has been improvement in our understanding of biochemical changes in response to mechanical forces and pathogenic infections in the periodontium, a significant gap of knowledge exits about how these disturbances regulate the differentiation of osteoblasts and osteoclasts. Therefore, we must further our understanding about the differentiation of osteoblasts from mesenchymal progenitor cells and osteoclasts form the hematopoietic/monocyte lineage.

1.2 Gingivitis and Periodontitis

1.2.1) Periodontal health

Before we can discuss diseases of the periodontium, we need an understanding of what periodontal health encompasses.

We must understand that periodontal disease is a multifactorial disease. The intricate interplay between the microbial biofilm, the host immune and inflammatory response, and environmental factors can maintain periodontal health or cause dysbiosis leading to periodontal disease.

Periodontal health can be defined at both a histological and clinical level. This will allow the clinician to have a reference point to be able to diagnose periodontal disease and present different therapeutics with their associated treatment outcomes to the patient.

Clinical studies have shown that healthy gingival tissues present with minimal inflammation reflected at sites with bleeding upon probing, no probing depths >3mm, no redness, edema, and pus[8].

These clinical finding have been mirrored in histological studies. These studies have shown that a clinical healthy gingiva has a connective tissue layer with minimal inflammatory cell infiltrate. Even with optimal oral hygiene, there is a small population of polymorphonuclear leukocytes in the connective tissue[9, 10]. Physiologically, their role is to function as surveillance cells to potential infections. Another histological characteristic of clinically healthy gingiva is a high volumetric density of collagen and fibroblasts.

1.2.2) Gingivitis

Histological studies in both animals and humans have shown that with the cessation of oral hygiene and plaque accumulation, the bacterial lipopolysaccharide (LPS) and metabolic products of the oral microbiome induce a host response. This results in the release of proinflammatory cytokines, various leukocytes and ultimately development of gingivitis.

In the early phases of plaque accumulation, polymorphonuclear neutrophils (PMNs) are the most abundant leukocytes and provide local defense against bacteria by forming a wall between the bacteria and tissues. With continued plaque accumulation, the bacterial infection penetrates deeper into connective tissue layer stimulating additional PMNs, macrophages, and lymphocytes to the site. Macrophages release many pro-inflammatory mediators such as cytokines, Prostaglandin E2 (PGE2), and Matrix Metalloproteinases (MMPs) which recruit additional immune cells to the site[11].

These histological changes are seen clinically as inflamed gingival tissues, the severity of which is dependent on the extend of and duration of plaque accumulation. Other clinical parameters include redness, probing depth ≥3mm with no attachment or bone loss, edema and/or pus.

In susceptible individuals, if the bacterial challenge is not controlled the pro-inflammatory mediators cause connective tissue and bone loss marking the progression of gingivitis to periodontitis.

1.2.3) Periodontitis

Periodontitis is a multifactorial chronic inflammatory disease of the periodontium (Fig. 6). The etiological factors are categorized into microbiological, host, and environmental factors[8] (Table 1). Periodontal disease is characterized by clinical attachment loss, alveolar bone loss,

deep probing depths, and gingivitis. At least 20-24% of Canadians, aged 20-79, have moderate to severe periodontal disease[12]. The consequences of periodontitis when left untreated can lead to tooth loss which has a negative impact on chewing function, esthetics, and quality of life. In addition, periodontal disease can have systemic implications by increasing the risk of cardiovascular disease, pulmonary disease, stroke, diabetes, and preterm birth[13].

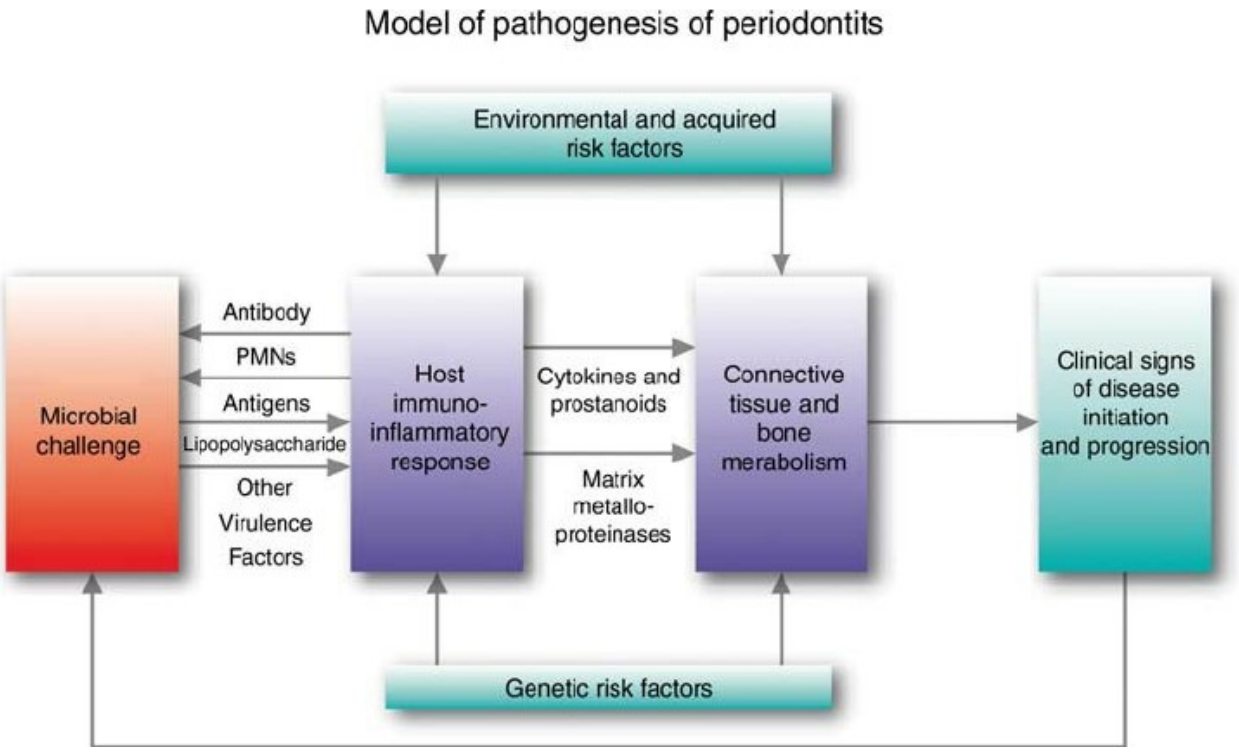

Figure 6: Pathogenesis of periodontitis. This model shows the multiple factors that influence the extend and severity of periodontitis[14].

Table 1: Etiological factors involved in Periodontal disease:

Microbiological factors	• Supragingival plaque • Subgingival plaque	
Host factors	**Local factors:** • Periodontal pockets • Dental restorations • Root anatomy • Tooth position and crowding	**Systemic factors:** • Host immune response • Systemic health • Genetics
Environmental factors	• Smoking • Medications • Stress • Nutrition	

With persistent gingivitis, the plaque biofilm grows laterally and apically along the root surface creating a microbiological environment necessary for periodontitis. In susceptible individuals, the shift from gingivitis to periodontitis represents a stage which the bacterial challenge has overwhelmed the immune system and any tissue repair is unlikely. The immune system in trying to contain the bacterial infection stimulates many pro-inflammatory mediators. For example, macrophages produce cytokines (TNF-α, IL-1, IL-6, IL-8, and IL-12), PGE2, and MMPs which

are responsible for the destruction of gingival connective tissue, periodontal ligament fiber, and alveolar bone[1] (Fig. 7).

Alveolar bone loss is a hallmark of periodontal disease which is mediated by osteoclasts. Osteoclasts are multinucleated cells derived from the hematopoietic/monocyte lineage capable of degrading the organic and inorganic components of bone. During periodontitis, a variety of mediators such as, PGE2, TNF-α, IL-1, IL-6, IL-11, IL-17, and IL-12 may active osteoclasts[1]. Another important signalling pathway involved in osteoclastogenesis includes receptor activator of nuclear factor-kappa beta (RANK), the RANK ligand (RANKL) and osteoprotegrin (OPG). When RANKL binds to RANK, a receptor found on osteoclasts precursors, it will induce osteoclast differentiation. The exact opposite happens when OPG bonds to RANKL. Some studies have shown a correlation between a higher level of RANKL expression, and a lower OPG level on periodontitis sites in comparison to healthy gingival tissues. These studies, however, could not distinguish between active versus periodontitis in a quiescence, thus pointing to the involvement of other regulatory pathways yet to be identified [15, 16].

There now exists a wealth of knowledge regarding the microbiology of periodontitis and its influence on many biochemical mechanisms involved in the gingivitis, connective tissue and bone destruction. However, there is still a lack of understanding with respect to the factors that govern the transition from gingivitis to periodontitis. Other factors that add to the complexity of periodontitis comprise of environmental factors plus the host's local and systemic factors. Currently, a great deal of research is underway to understand the complex interplay of the microbiological, host, and environmental factors triggering the shift from gingivitis to

periodontitis with the ultimate goal of finding therapeutic concepts to prevent connective tissue loss and bone loss.

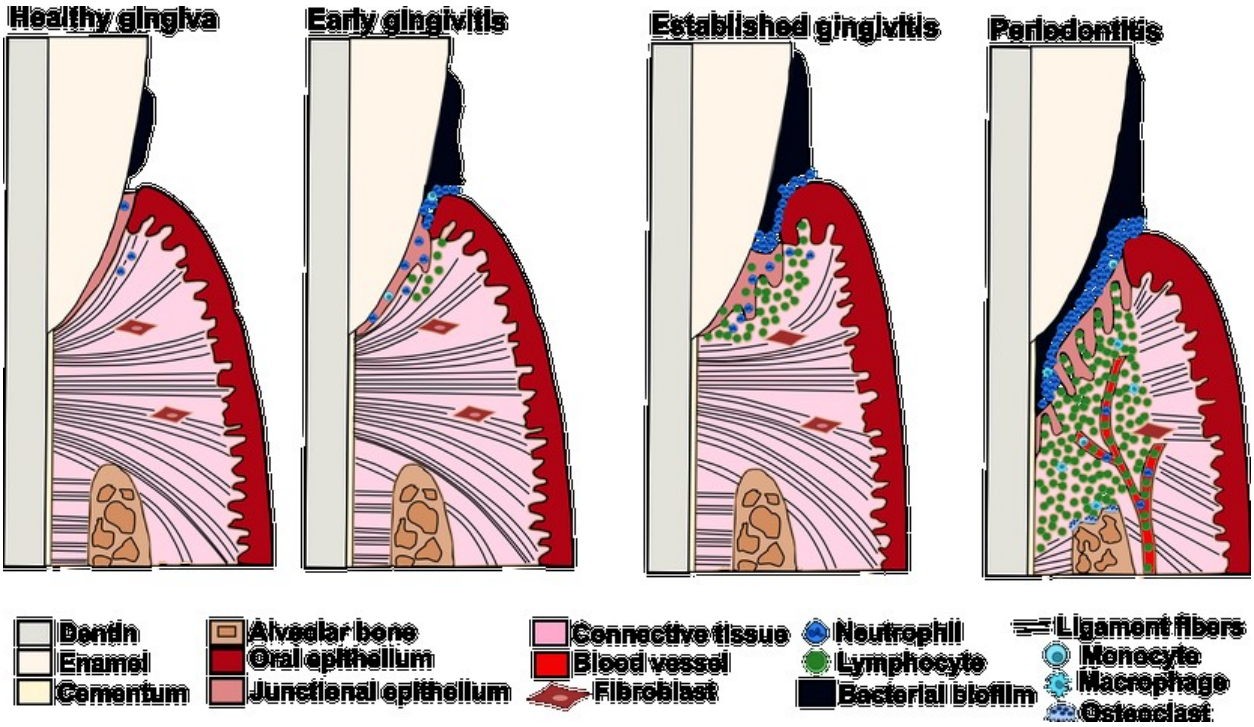

Figure 7: Schematic showing the progression of gingivitis to periodontitis. With inadequate plaque control, the microbial biofilm stimulates an array of proinflammatory cytokines and activation of the immune system. This leads to Gingivitis, a reversible inflammatory condition involving only the gingival tissues, without damage to the attachment apparatus (cementum, periodontal ligament, alveolar bone). In some individuals, gingivitis progress to periodontist if not managed. This is characterized by damage and loss of the attachment apparatus. Adopted from https://fuzzytoothsweater.wordpress.com/2016/04/18/this-is-why-flossing-is-important.

1.3) Bone as a Living Tissue

The skeletal system in an adult body is made up of 206 individual bones providing mechanical support and locomotion. However, bone tissues serve other functions including protection of vital organs (internal organs, brain, and spinal cord), support and anchorage of teeth into the maxilla and mandible, providing a source for hematopoietic stem cells present in the bone, and a reservoir of minerals utilized to achieve systemic homeostasis[1].

During embryonic development, the human skeleton forms from paraxial somitic mesoderm and neural crest-derived mesoderm of the branchial arches and subsequently undergo ossification via intramembranous or endochondoral ossification[17].

The cranial vault, maxilla, and mandible form through intramembranous ossification where connective tissue serves as the scaffold upon which new bone matrix is laid down. In contrast, the remaining bones of the body go through endochondral ossification where cartilage serves as a template only to be completely replaced with bone[1].

Once bone has formed, it undergoes modeling and remodeling. Modeling causes a change in the initial architecture of bone whereas remodeling causes a change in the mineralized component of bone without affecting the overall shape or form[1]. These processes are important for bone repair, growth and differentiation.

In recent years, studies have identified many growth factors are involved in the regenerative/remodeling phase of bone wound healing (Table 2)[1]. Growth factors are biological mediators that bind to cell surface receptors to activate intracellular signalling pathways leading to gene expression and changes in cellular activity and phenotype.

Table 2: Growth factors involved in bone resorption and bone apposition

Growth factor	Cell of origin	Function
BMPs 2-4	Osteoblasts	Stimulates mesenchymal progenitor cell migration
BMP-7	Osteoblasts	Stimulates osteoblast and chondroblast differentiation
FGF-2	Macrophages, Endothelial cells	Stimulates mesenchymal progenitor cell migration
IGF-II	Macrophages, Fibroblasts	Stimulates osteoblast proliferation and bone matrix synthesis
PDGF	Macrophages, Osteoblasts	Stimulates differentiation of fibroblasts into myofibroblasts Stimulates proliferation of mesenchymal progenitor cells
TGF-β	Fibroblasts, Osteoblasts	Induces endothelial cell and fibroblast apoptosis Induces differentiation of fibroblasts into myofibroblasts Stimulates chemotaxis and survival of osteoblasts
VEGF	Macrophages	Chemotaxis of mesenchymal stem cells, antiapoptotic effect on the bone forming cells, angiogenesis promotion

*BMP = bone morphogenetic protein, FGF = fibroblast growth factor, IGF = insulin-like growth factor, PDGF = platelet-derived growth factor, TGF = transforming growth factor, VEGF = vascular endothelial growth factor.

The alveolar bone as part of the periodontium experiences modeling and remodeling like any other bone tissue within the body. For example, when alveolar bone is lost due to trauma, infectious diseases (periodontitis) and/or surgical interventions; the remodeling process is activated as part of the wound healing process to restore balance and strength within the tissue. Furthermore, these processes are involved during regenerative therapies to promote new bone formation and osteointegration after dental implant placement.

1.4) Mechanisms and Pathways involved in Bone Remodeling

The human skeletal framework is composed of an inorganic matrix mainly hydroxyapatite (Ca10 [PO4]6[OH]2) and an organic component consisting mainly of type I collagen[18]. During development and throughout life, our bones act as dynamic connective tissues constantly undergoing physiological remodeling which involves the replacement of old or damaged bone with new bone matrix. The major players in this process are osteoclasts and osteoblasts.

1.4.1) Osteoclasts and Osteoblasts

The cells involved in the remodeling process are called osteoclasts and osteoblasts.

Osteoclasts are multinucleated cells responsible for the resorption of old or damaged bone. They are derived from hematopoietic stem cells and form by fusion of mononuclear progenitors of monocytes/macrophages. The major transcriptional factor, Nuclear Factor of Activated T-cells cytoplasmic 1 (NFATc1), is required for the differentiation and functioning of osteoclasts[18]. A differentiated and functioning osteoclast degrades the bone matrix by attaching to the bone surface and secreting lysosomal enzymes and hydrogen and chloride ions. This creates a concavity called the Howship lacunae.

Osteoblasts are derived from pluripotent mesenchymal progenitor cells which can differentiate into adipocytes, myocytes, chondrocytes, or osteoblasts[18]. Differentiating into the osteoblast lineage requires the expression of transcription factors: Runt-Related Transcription Factor 2 (RUNX2) and Osterix (Osx)[19, 20]. A mature osteoblast is responsible for the deposition and mineralization of new bone matrix in the Howship lacunae.

1.4.2) Bone Resorption and Bone formation

Bone remodeling is the response to internal and external stimuli, which ensures an intact bone architecture necessary for functional demand throughout life.

The remodeling cycle is composed of five phases: activation, resorption, reversal, formation, and termination[21] (Fig. 8).

Activation phase: Osteoclast precursor cells (mononuclear monocyte/macrophage cells) are recruited from the circulation to the site of resorption where they will fuse together and differentiate into an osteoclast.

Resorption phase: Consists of morphological changes within the osteoclast cytoskeleton, attachment to the bone surface, and formation of a ruffled border which provides a greater secretory surface area. The H+-ATPase pump located at the ruffled border pumps hydrogen ions into the resorption lacunae to degrade the bone minerals. In addition, proteases such as Cathepsin K and matrix metalloproteinases secreted at the ruffle borer help to degrade organic component of bone. Once resorption is complete, osteoclasts undergo apoptosis to prevent excessive bone resorption.

Reversal phase: Involves the transition from bone resorption to bone deposition, the exact nature of which is currently poorly understood. Studies have shown that the Howship lacunae is mostly covered with mononucleated cells called reversal cells which appear after the departure of osteoclasts and before the arrival of osteoblasts. This suggests that reversal cells act as an intermediate mediator between osteoclasts and osteoblasts. It has been proposed that reversal cells prepare the Howship lacunae for osteoblasts by receiving and/or generating signals which couple bone resorption to bone formation[22].

Formation phase: Once osteoblasts reach the resorption site; they secret a type I collagen-rich osteoid matrix which serves as the scaffold for the mineralization of the bone matrix. This mineralization process which includes hydroxyapatite crystal deposition at collagen fibrils is poorly understood.

Termination phase: After the mineralization of the bone matrix, the osteoblasts can either differentiate into osteocytes entrapped within the bone matrix, remain on the bone surface as bone lining cells, or undergo apoptosis.

Bone remodelling is a highly regulated lifelong process which replaces approximately 10% of the human skeletal bones annually[23]. This allows for maintenance of bone integrity, repair of damaged bone, and mineral homeostasis.

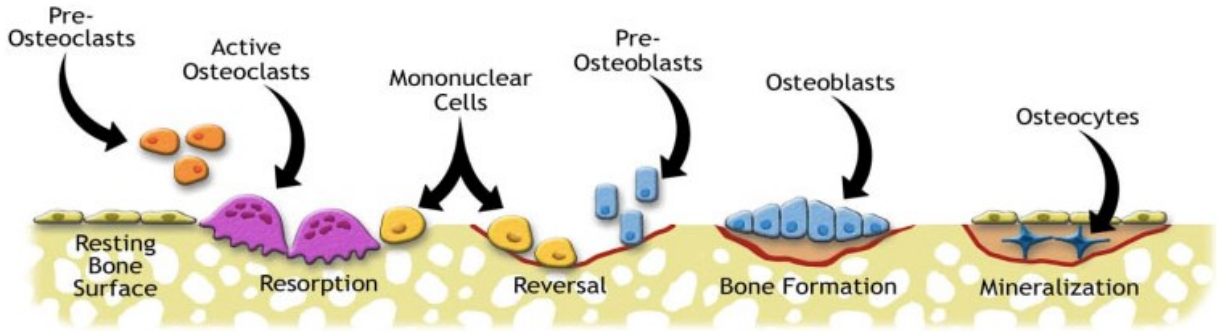

Figure 8: Schematic showing the bone remodeling process. Preosteoclasts are recruited to sites of resorption and differentiate into active osteoclasts. They release protons and proteases necessary for bone resorption. Once bone resorption is completed, preosteoblasts are recruited to these sites, differentiated int active osteoblasts, and secrete new bone matrix. Once mineralization is complete, some osteoblasts become entrapped in the bone matrix as osteocytes. https://www.orthopaedicsone.com/display/Clerkship/Describe+the+process+of+bone+remodeling.

1.5) Osteoclastogenesis

Osteoclasts are the end product of a terminally differentiated myeloid precursor cell. This is a highly regulated process involving cytokines, bone cells, and immune cells. The signals from the regulatory bodies must be coordinated to allow myeloid precursor proliferation, fusion into multinucleated cells, cellular polarization, bone adherence, and functional bone resorption[18].

1.5.1) The RANK/RANKL/OPG system

The two most important stimuli for osteoclastogenesis are the macrophage colony stimulating factor (M-CSF) and the receptor for activation of nuclear factor kappa B ligand (RANKL)[24, 25](Fig. 9).

The main source of M-CSF are osteoblasts, stromal cells, and osteoctyes. Its primary function includes the proliferation and survival of myeloid precursor cells by binding to its receptor, Colony Stimulating Factor Receptor 1 (c-Fms) and upregulating the RANK receptor on these precursor cells[18].

In a study by Kodama, osteopetrotic (op/op) mice were injected with recombinant M-CSF and examined. These mice have a deficiency in MCSF production due to a mutation within the M-CSF gene and as a result have osteopetrosis. The results showed many osteoclasts on the long bones which cured the osteopetrosis in these mice demonstrating that M-CSF is one of the factors required for osteoclastogenesis[25].

RANKL is part of the tumor necrosis factor cytokine family and it is an essential cytokine is the differentiation of osteoclasts. RANKL is expressed by osteoblasts, stromal cells, osteocytes, B-cells and T-cells[18]. When RANKL binds to RANK on myeloid precursor cells it stimulates these precursor cells to differentiate into mature multinucleated osteoclasts. Several studies have shown that mice with genetically deficient RANK or RANKL have few or no functioning

osteoclasts and as a result experience osteopetrosis. Another observation was that teeth failed to erupt in these mice because of the lack of osteoclasts responsible for resorption of the bone overlying the teeth[26-29].

Although both M-CSF and RANKL are needed for osteoclasts differentiation, it is RANKL that is required for osteoclast survival and osteoclastic bone resorption[30].

Osteoprotegerin (OPG) is another cytokine from TNF family which has an inhibitory effect on osteoclast differentiation and activation. It acts as a soluble decoy receptor for RANKL. It prevents RANKL from binding to RANK which inhibits osteoclast differentiation. This has been confirmed by studying OPG deficient mice and mice that overexpress OPG. In the former, osteoporotic bone was observed while the latter exhibited osteopetrotic bone[31, 32].

The expression of RANKL and OPG is under the influence of hormones, cytokines, and growth factors. These local and systemic factors have an indirect effect on osteoclast differentiation by regulating the expression of RANKL and OPG expression in osteoblasts. Therefore, the ratio of RANKL and OPG that is present around osteoclast precursor cells controls the amount/extent of osteoclast differentiation.

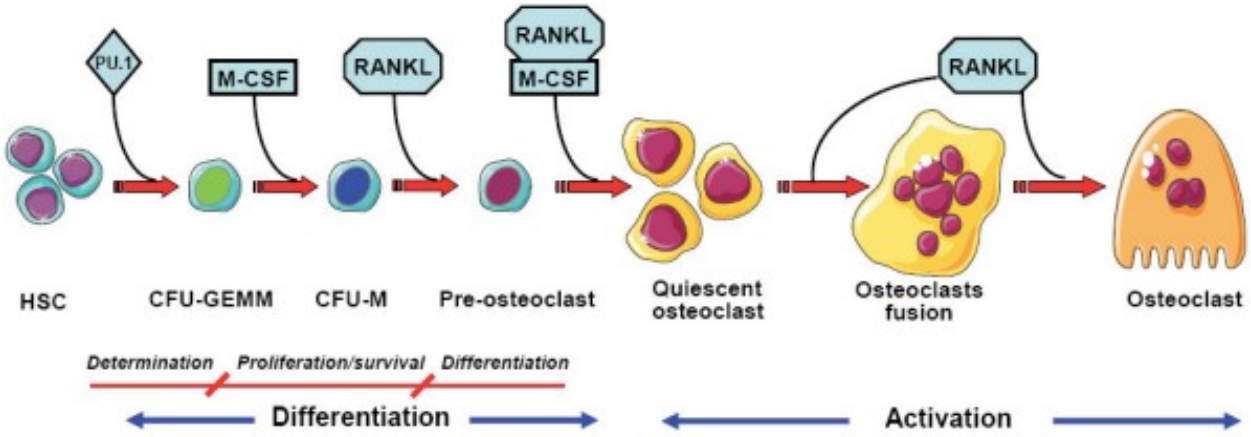

Figure 9: Schematic showing osteoclastogenesis. Hematopoietic cells in the presence of MCSF and RANKL differentiate into active multinucleated osteoclasts. OPG acts as a negative regulator of osteoclastogenesis. OPG binds to RANKL, preventing it a from binding to its receptor. HSC: Hematopoietic cells, MCSF: macrophage colony stimulating factor, RANKL: Receptor activator of nuclear factor kappa-B ligand, OPG: Osteoprotegerin.[33]

1.5.2) Formation of Multinucleated Osteoclasts

Multinucleation is a unique property of osteoclasts which occurs through fusion of multiple pre-osteoclastic cells. The binding of RANKL to its receptor causes the stimulation of three transmembrane proteins involved in osteoclast fusion. These proteins are known as DC-STAMP and OC-STAMP (dendritic cell- and osteoclast- specific transmembrane protein) and ATP6V0d2 (ATPase, H+ transporting, lysosomal 38 kDa, V0 subunit d2)[18]. A deficiency in any of these three proteins will result in a defective osteoclast incapable of bone resorption[34-36].

The binding of RANKL leads to the upregulation of NFATc1/NFAT2 and c-fos transcription factors necessary for osteoclast development. It has been recognized that NFATc1 is the master transcription factor in osteoclastogenesis and embryonic stem cells deficient in NFATc1 failed to develop osteoclasts[37]. The RANKL-RANK mediated expression of these transcription factors induces the expression of several genes that define an osteoclast. These genes include TRAP, integrin β3, cathepsin K, matrix metalloprotease 9, and calcitonin receptor[38].

1.5.3) Bone Resorption

Mature osteoclasts are highly motile cells capable of migrating to resorption sites via cytokines released from osteoblasts[39]. Upon arrival at these sites, the intra-cellular morphology of osteoclasts becomes polarized to allow for attachment and resorption of bone. The apical end is in close proximity of the bone surface and consists of lyozymes and mitochondria. While the basolateral side houses the Golgi apparatus, the rough endoplasmic reticulum, and the nucleus. The apical structures produce degrading enzymes to resorb bone and the basolateral structures are responsible for transferring the resorption products into the main circulation[40-42].

An active resorbing osteoclast can be divided into 3 domains: the sealing zone, the ruffled border, and the functional secretory domain[18].

The sealing zone provides the attachment of osteoclasts onto the bone surface. This is accomplished by tight adhesions called podosome rings which consists of actin microfilaments and integrins[43]. This attachment forms the Howship or resorption lacuna.

The ruffled border is positioned central to the sealing zones with the primary role of secreting protons and digestive enzymes to degrade the bone matrix. The V-HATPase is located in the ruffled border plasma membrane which pumps protons into the Howship lacuna. The degradative enzymes packaged into lysosomes (cathepsin K, TRAP, and matrix metalloproteinases (MMPs)) are released into Howship lacuna via fusion of the lysosomal membrane with the ruffled border[18]. Once the bone matrix is dissolved, the osteoclast re-uptakes the by-products through the ruffled border. The basolateral structures which make up the functional secretory domain packages the by-products and transports them into the main circulation[40](Fig. 10).

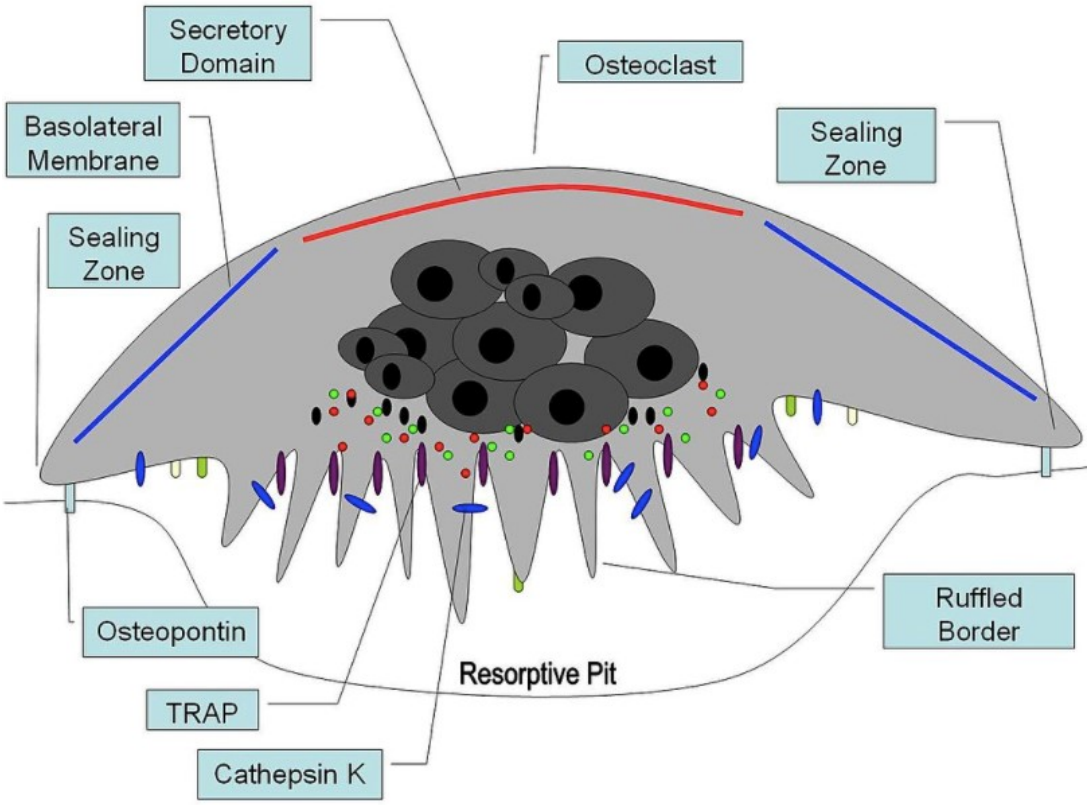

Figure 10: Schematic showing a polarized active osteoclast. An active osteoclast has 3 zones: Sealing zone provides the attachment to the bone surface via podosomes. The ruffled border is the site of proton and protease secretion causing bone resorption. The functional secretory domain packages the resorption by-products and sends them into the main circulation. From: https://en.wikipedia.org/wiki/Osteoclast#/media/File:Osteoclast1.jpg

1.6) Bone Morphogenetic Proteins Signalling

Bone morphogenic proteins are growth factors with a diverse function effecting many tissues throughout the body. They participate in the formation and regulation of angiogenesis, neurogenesis, muscle homeostasis, heart formation, bone, cartilage, tendon, tooth formation, immune function and many more[44]. Bone morphogenic proteins belong to the transforming growth factor beta (TGFβ) family. Currently, studies have identified 12 different BMPs

functioning as important signalling molecules involved in various biological processes[45]. With respect to bone remodelling, several BMPs (BMP 1, 2, 4, 6, 7) have shown osteoinductive properties. These BMPs stimulate mesenchymal progenitor cells to differentiate into osteoblasts which are the principal cells in bone formation[1]. However, in recent years the effect of BMPs on bone resorption has gained considerable attention. Studies show that the same BMPs that induced bone formation via osteoblasts are also responsible for bone resorption via osteoclasts. In particular BMP2 and 4, have highly osteogenic properties but also cause bone resorption by stimulating osteoclast differentiation [46, 47]. It must be noted that BMPs are under the control of their antagonist which restricts BMP signalling (Fig. 11)[48].

Studies have shown that mice deficient in Twisted gastrulation had increased number of osteoclasts causing more bone loss[49] while an overexpression of Twisted gastrulation led to an increase in bone mass[50].

In another study by Graf et al., several BMPs and BMP antagonists which were expressed in healthy periodontal tissues had a dynamic change in expression levels during the course of periodontal disease[51].

From these studies we can conclude that BMPs act as an important mediator during bone remodelling as it is involved in the formation of both osteoblasts and osteoclasts.

By understanding the effects of BMPs and their antagonists on bone remodeling, we can develop and improve new therapeutic approaches to facilitate bone fracture repair.

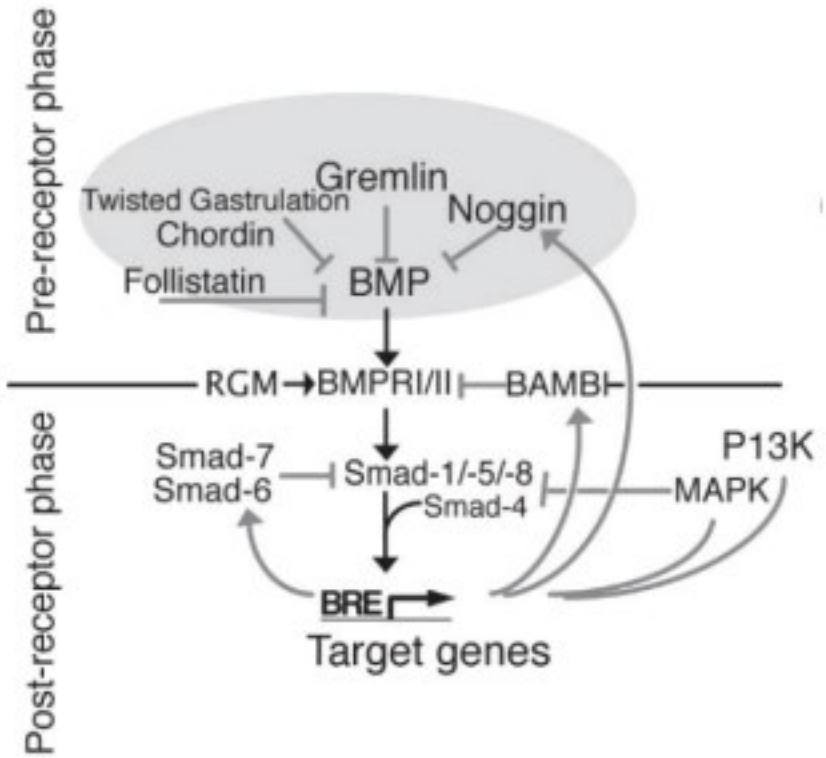

Figure 11: Schematic of BMP signaling pathway indicating how secreted BMP antagonists control to which cells BMP molecules can signal. Grey circle: antagonists, grey arrows: blocking action[48].

1.7) BMP2 and its Antagonist

The osteoinductive capability of BMPs has opened the door for the use of these growth factors in a variety of clinical situations with the goal of promoting bone formation. For instance, Recombinant BMP2, is used for alveolar bone augmentation[52]. However, other studies have uncovered the diverse role of BMP2 in promoting osteoclast differentiation (bone resorption)[47], attracting and controlling differentiation of macrophages (inflammation)[53], and contributing to the formation of the periodontal tissues[54-56]. All these functions can occur in the periodontium which means BMP2 is secreted within the extracellular matrix to influence

these processes while its signalling activity is locally controlled by its antagonist. These antagonists include: Gremlin1 (GRM1), Chordin (CHRD), and Twisted Gastrulation (TWSG1). Due to the complex and interactive functionality of BMP2, the clinic success of recombinant BMP2 in bone healing has been unpredictable. Therefore, we need a detailed understanding regarding the nature of BMP2 and its antagonists in affected tissues in order to take advantage of its full potential as a therapeutic approach for bone healing.

1.8) BMP in a Periodontal Damage Model

In a study by Graf et al., the expression of various BMPs and BMP antagonists was seen in healthy periodontal tissues which dynamically changes during the course of periodontal damage. In this study, silk ligature model [57] was used in lacZ reporter mice to induce periodontal damage and the expression of BMP2, BMP7, TWSG1, GRM1 and CHRD was assessed at days 3, 5, 8, and 15. The silk ligature is tied to the second molar for rapid accumulation of plaque and bacteria causing inflammation and subsequent bone loss. The results showed that the expression of BMP/BMP antagonists is changed following ligature placement. In particular, the expression of CHRD increased from day 5 to day 15 with the progression of periodontal damage (Fig. 12). In addition, 8 days after ligature placement there was BMP2 and TWSG1 expression presumably at site of alveolar bone resorption as well as acellular cementum, periodontal ligament space and around osteocytes. However, CHRD was only seen around the alveolar bone presumably at resorptive sites (Fig. 13).

From this study, we can assume that the expression of BMP2 along with its antagonists CHRD and TSWG1 along the alveolar bone during periodontal damage may be suggestive of their involvement in both osteoclastogenesis and bone resorption in vivo.

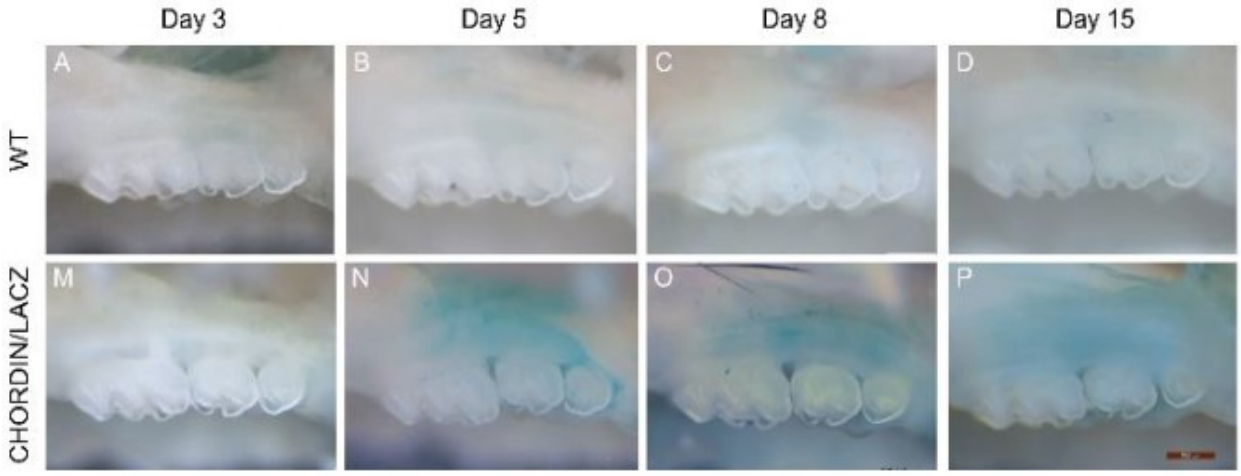

Figure 12: Chordin starts being expressed 5 days following ligature placement. Buccal view of wholemount stained Chordin LacZ reporter or control WT mice (n=3 per time point)[51].

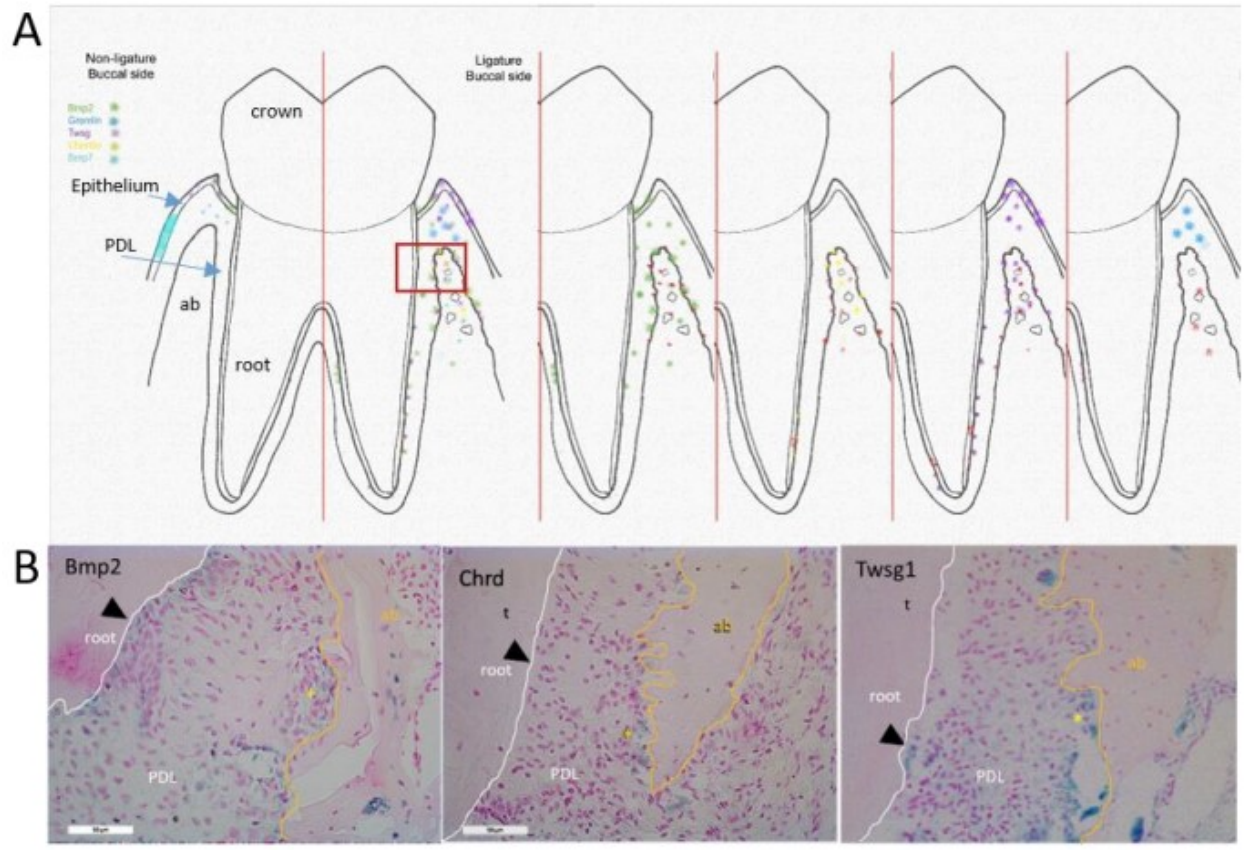

Figure 13: A: Schematic of BMP/BMP antagonist expression in healthy (left half of tooth) or 8 days following ligature placement (right half of tooth). For clarity, right half is repeatedly shown for the various genes in relation to TRAP+ cells, which indicate sites of bone resorption.
B: Paraffin section of lacZ stained tissue counterstained with nuclear fast red reporting expression (blue) of BMP2 (left), CHRD (middle), TWSG1 (right). BMP2 and TWSG1 are observed at the acellular cementum (arrowhead) covering the tooth (t, white line). BMP2 expression is also observed in osteocytes in the alveolar bone (ab, orange line). BMP2, TWSG1 and CHRD are all observed at sites of bone resorption (yellow star). Note restricted expression of CHRD in comparison to BMP2 or TWSG1. Ab=alveolar bone (orange), root (white), PDL=periodontal ligament[51].

1.9) The Role of BMP2 and its Antagonists on Osteoclastogenesis

Although it has been well established that BMP signalling is involved in the activation of osteoblasts and bone formation, their effect on osteoclasts is not fully understood. A growing number of studies suggest that osteoclasts have BMP receptors and that BMPs directly influence the differentiation and activity of osteoclasts[58-61]. There are various proteins in the extracellular matrix which regulate BMP signaling by competitively binding to BMPs preventing them from binding to their receptors. These antagonists include Chordin, Noggin, and Twisted Gastrulation[62].

In a study by Jensen et al., it was shown that in the presence of RANKL, BMP2 directly affects in vitro differentiation of osteoclasts. In contrast, when noggin was introduced to murine bone marrow cells, it had an inhibitory effect on osteoclast differentiation[47].

Moreover, in a study by Rodriguez et al. there was a reduction in bone density in Twisted gastrulation deficient mice due to increased BMP signalling on osteoclasts[49].

Interestingly, Chordin only inhibits BMP-2,-4, and-7[63]. With regards to osteogenesis, there seems to be a limited expression of chordin by osteoblasts and hence limited effect on osteoblastic function[64]. On the other hand, the expression of chordin and their effect on osteoclasts is not well known.

An interesting signalling network involving BMP2/CHRD/TWSG1 has been shown by Graf et al., where BMP-2/4 inhibits the development of thymocytes[65]. However, when thymocytes receive a signal via pre-TCR (T-cell receptor), they secrete TWSG1 which conjointly with CHRD removes the inhibitory action of BMP-2 resulting in thymocyte maturation (Fig. 14).

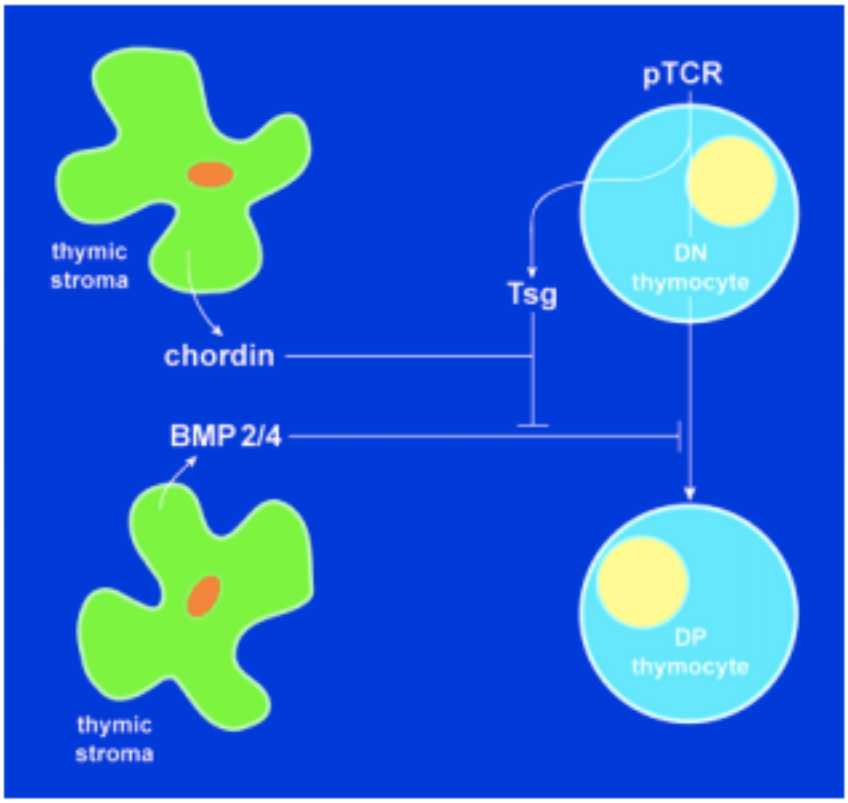

Figure 14: Development of thymocytes is regulated by a BMP/CHRD/TWSG1 signaling network. Twisted Gastrulation (Tsg) is induced following pTCR signaling, which acts in synergy with Chordin and allows the thymocyte to overcome a BMP2/4 block[65].

We have previously discussed the periodontal damage model (Fig. 13) where BMP2, CHRD, and TWSG1 are expressed in close proximity at the sites of bone resorption, suggesting the existence of a similar regulatory signalling network as seen during thymocyte maturation. Whether BMP signalling increases osteoclast differentiation directly or through the expression of transcription factors such as NFATc1 is an area requiring further research. In addition, it's been hypothesized that when osteoclasts resorb bone, they signal osteoblasts to synthesize new bone ensuring normal physiological bone remodeling[47]. As we have discussed, BMPs are important

regulators of bone formation, therefore it is of interest to investigate if BMPs expressed by osteoclasts are involved in the coupling of osteoclast to osteoblast activity.

In order to understand the role of individual components of the BMP signaling network in periodontal tissue, bone remodeling, and osteoclast maturation, we can take advantage of a newly developed CHRD KO mouse. Chordin is encoded by 23 exons that span a relatively small genomic region of only 10 kb. In this mouse, the CHRD coding exons 3-23 have been replaced by a LacZ reporter gene designed to be splice in frame to exon 2 of CHRD (Fig. 15, 16, Daniel Graf, unpublished). This mouse was made in collaboration with Regeneron Pharmaceuticals and remains unpublished.

In conclusion, in order to understand the role of BMPs on bone remodelling, we must also understand the factors involved in regulating BMPs in the local tissue. This will give rise to a novel signalling network which allows the current BMP therapeutic applications to be modified in better ways to manage diseases such as osteoporosis and periodontal disease by promoting bone regeneration.

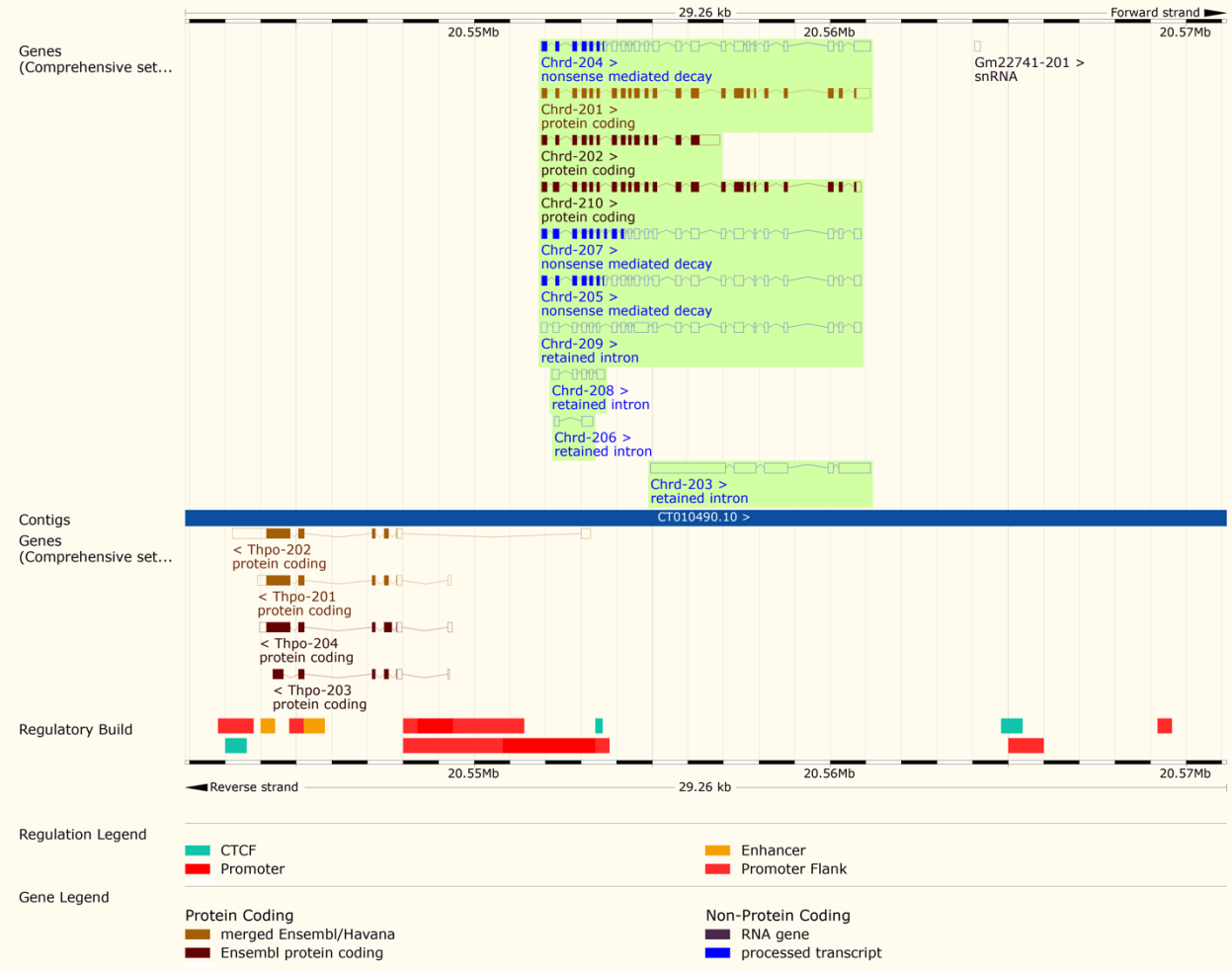

Figure 15: Schematic representation of the mouse CHRD genomic locus. CHRD is encoded on the proximal long arm of mouse chromosome 16 by 23 exons (green highlight) sharing regulatory regions (red boxes) with Thrombopoietin (Thpo, encoded on opposite strand).

A

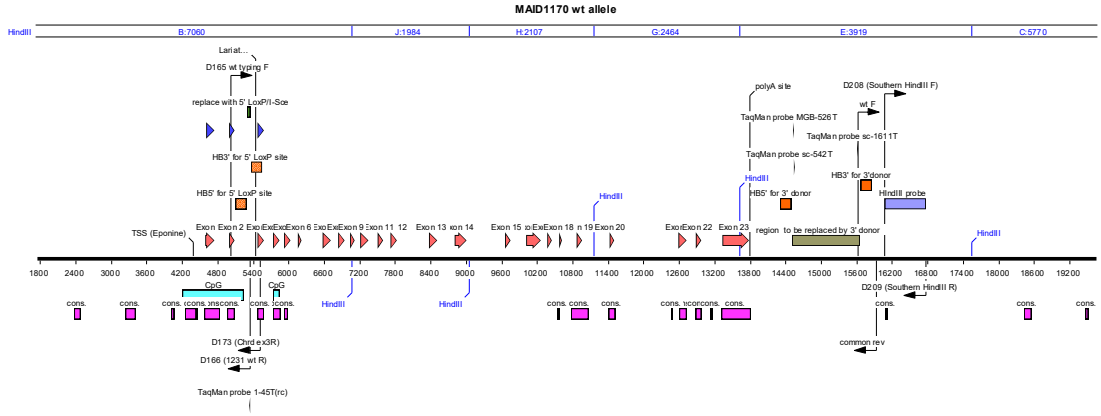

B

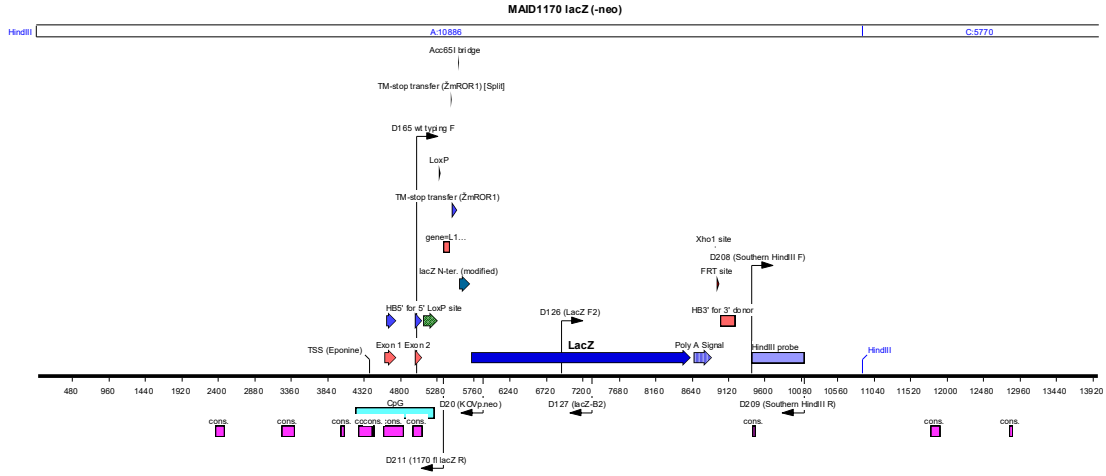

Figure 16: Schematic representation of gene targeting strategy of mouse CHRD genomic locus. CHRD exons are indicated by red arrow heads. A) placement of 5' loxP site (green bar) between exons 2 and 3 as well as the region to be replaced by the lacZ reporter gene (olive box). B) CHRD lacZ reporter construct following loxP recombination showing exons 1-2 (red arrows), loxP site (green arrow), lacZ reporter gene (blue arrow). Expression from the targeted CHRD locus will result in expression of a CHRD-lacZ reporter product used to map expression of CHRD (compare to Fig. 14). All data regarding the CHRD mutant mouse remain unpublished.

Chapter 2: Aims and Hypothesis

Currently it is accepted that osteoclast differentiation is dependent on the binding of RANKL secreted by osteoblast precursor cells to the RANK receptor on osteoclasts. The data from Graf et al., indicates that BMP2/TWSG1/CHRD might provide a second regulatory network for osteoclastogenesis[51]. In support of this, BMP2 synergizes with RANKL to induce osteoclast differentiation in vitro[47] and TWSG1-deficient mice show increased osteoclast formation and osteopenia[49]. As TWSG1 cannot function as a BMP antagonist in the absence of CHRD, we propose that CHRD expression observed in the vicinity of osteoclasts in the periodontal tissue is critical to restrict local BMP2 action on osteoclasts.

The focus of this study will be on BMP2 and its antagonist CHORDIN (CHRD) in healthy and damaged periodontal tissue with the following objectives:

OBJECTIVE 1: Characterizing how BMP2/CHRD interact during osteoclast maturation in vitro
OBJECTIVE 2: Assessing the role of CHRD in osteoclast differentiation in vitro

We hypothesize that CHRD restricts BMP2 induced osteoclasts differentiation, possibly through regulation of osteoclast fusion, resulting in a reduction of generated osteoclasts.

Chapter 3: Materials and Methods

Mice

This protocol was approved by the University of Alberta Animal Care and Use Committee protocol 1648 with accordance to the recommendations of the Canadian Council on Animal Care. All mice had been backcrossed for at least 10 generations to C57l6/J. For genotyping, genomic DNA was extracted from tissue biopsies (ear punches or distal phalange biopsy) using Proteinase K digest followed by phenol extraction. The genotypes were documented by PCR on genomic DNA using the following primer strategy: D165: (5' ATGCCTTGGACGAGACGTGG 3'), D166 (5' AACTTCTCTGAGCCTCGGCGTC 3'), D219 (5'-CCACACTTGGCACCAGAATG -3') resulting in products of 343bp (wt allele, D165/D166), 474bp (lacZ reporter allele, D165, D219).

Mouse Bone Marrow Cell Culture

Bone marrow mononuclear cells were collected from 2 – 8 months old WT mice with C57Bl6 background and CHRD KO mice. The mice were euthanized by cervical dislocation in accordance with institutional guidelines. The femurs and tibias were dissected, and all adhering tissues were removed in sterile conditions. All bones were placed in a tissue culture dish. To preserve cell viability, the bones were kept in these conditions for less than 1 h.

Isolation:

The bone ends were cut off with scissors and the marrow cavity was flushed with minimum essential medium (α-MEM) using a sterile 25 G needle. The bone cavities were flushed multiple times from both ends until the bones appeared pale white. The bone marrow contents were flushed into 15ml tubes and centrifuged at 1200 RPM at room temperature for 5 minutes. The

supernatant was aspirated. If there was a heavy contamination of red blood cells (RBC) in the bone marrow, the cell pellets were gently resuspended and treated with 1 mL of red blood cell lysis buffer. After 1 minute, phosphate buffered saline PBS (14ml) was added to dilute the RBC lysis buffer. The tubes were again centrifuged at 1200 RPM at room temperature for 5 minutes. The supernatant was aspirated. The cell pellets were resuspended in 6 ml of α-MEM supplemented with 10% fetal bovine serum (FBS), 1% penicillin-streptomycin and 1% glutamine and cultured in a 25 cm^2 tissue culture flask. The tissue culture flasks were placed in 37 °C in a 5% CO_2 incubator overnight.

Plating and Initial induction with MCSF (Day -3):

For the first set of experiments, all non-adherent cells from WT mice were removed the following day and seeded at 2 x 10^5 cells/well. While the second set of experiments utilizing WT and CHRD KO mice, all non-adherent cells were seeded at either 2 x 10^5 cells/well (low density) or 4 x 10^5 cells/well (high density) in a 48 well plate. All cells were cultured in 400ul of α-MEM supplemented with 10% FBS, 1% penicillin-streptomycin, 1% glutamine, and M-CSF (30 ng/ml). The plates were placed in 37 °C in a 5% CO_2 incubator for 3 days.

RANKL induction (Day 0):

After 3 days of preincubation with M-CSF, the medium was aspirated and replaced with new medium:

- Half of the cells were cultured in 400 ul of α-MEM supplemented with 10% FBS, 1% penicillin-streptomycin, 1% glutamine, and M-CSF (30 ng/ml).
- The other half were cultured in 400 ul of α-MEM supplemented with 10% FBS, 1% penicillin-streptomycin, 1% glutamine, M-CSF (30 ng/ml), and RANKL (50 ng/ml).

A total of 4 plates were used, each representing a different time point during the first set of experiments with WT mice:

- Plate 1: Day 2 post RANKL induction
- Plate 2: Day 4 post RANKL induction
- Plate 3: Day 6 post RANKL induction
- Plate 4: Day 8 post RANKL induction

A total of 2 plates were used, each representing a different time point during the second set of experiments using WT and CHRD KO mice:

- Plate 1: Day 4 post RANKL induction
- Plate 2: Day 8 post RANKL induction

The medium in all plates were replaced every other day until day 8 which marked the end of the experiment. At each time point, cells were fixed with 4% paraformaldehyde (PFA) for TRAP staining which allowed for the quantification of osteoclasts. In addition, total ribonucleic acid (RNA) was extracted at each time point for gene expression by quantitative reverse transcription polymerase chain reaction (qRT-PCR). All plates were maintained at 37°C in 5% CO_2 incubator.

4% Paraformaldehyde (PFA)

1. Measure paraformaldehyde and add in 1 L bottle using funnel (see formula table below)
2. Heat H2O (MilliQ water) in 2000 ml beaker to 60°C (use the microwave oven ~5 min for 800 mL)
3. Add the heated H2O in 1 L bottle containing paraformaldehyde.
4. Put a magnet inside the bottle and put the bottle on a hotplate.

5. Add 1M NaOH into the bottle to dissolve PFA (see formula table below).
6. The solution will turn into a transparent solution when PFA is dissolved. If PFA is not completely dissolved, add more 1M NaOH drop by drop until the solution gets transparent.
7. Add 10X PBS into the solution (add PBS only once the PFA is completely dissolved).
8. Remove the bottle from the hot plate and fill up to 1000 ml with MilliQ H2O. The pH should be ~7.4.
9. Aliquot in 50 ml falcon tubes and freeze at -20°C for long-term storage.

IMPORTANT: The paraformaldehyde powder is extremely toxic, heated H2O should only be added to it in the fume hood.

Formula:

Total volume	MilliQ H2O (starting volume)	Paraformaldehyde (PFA)	NaOH (1M)	10X PBS *add after PFA is dissolved
250ml	200ml	10g	100µl	25ml
500ml	400ml	20g	200µl	50ml
1000ml	800ml	40g	400µl	100ml

1X Phosphate Buffered Saline (PBS)

Reagents/Apparatus	Supplier	Cat#	Storage/location
MilliQ water	-	-	MilliQ machine
NaCl, Mw 58.44	Fisher	BP358-212	Shelf 7-108A
KCl, Mw 74.55	Sigma	P9541	Shelf 7-108A
Na2HPO4 anhydrous, Mw 141.96	Sigma	71640	Shelf 7-108A
KH2PO4, Mw 136.08	Fisher	P285	Shelf 7-108A

For 1 L:
80 g NaCl (Fisher cat# BP358-212)
2 g KCl (Sigma cat# P9541)
14.4 g Na2HPO4 anhydrous (Sigma cat# 71640)
2.4 g KH2PO4 (Fisher cat# P285)
MilliQ water

1. Combine NaCl, KCl, Na2HPO4 and KH2PO4.
2. Add 800 mL MilliQ water. Mix well to dissolve.
3. Adjust volume to 1 L by adding MilliQ water. This will result in 10X PBS.
4. Check pH - should be about 6.8. Adjust using 10M NaOH or HCl if necessary.
5. Sterilize by autoclaving. Store at room temperature.
6. Add 100mL 10X PBS to 900 mL MilliQ water.

Tartrate-resistant acid phosphatase (TRAP) staining

At each time point a number of wells were assigned for TRAP staining according to the following protocol:

1. The medium was aspirated and washed 2 times with 1ml PBS being careful to not contact the bottom of the well.
2. The cells were fixed using 300ul 4% PFA in the wells for 5 minutes.
3. The PFA was aspirated and a 2-times wash with PBS was performed begin careful not to contact the bottom of the well.
4. The final wash with PBS was not aspirated. A parafilm was used to cover the plate, which was then stored in 4°C fridge.
5. The TRAP staining solution was made using TRAP basic incubation solution, Fast-Red Violet LB Salt, and Naphtol AS-MX phosphate. The Fast-Red Violet LB Salt must be dissolved in the mix before proceeding to the next step.
6. The PBS in the wells were removed and 400ul of TRAP staining solution mix was added to each well.

7. The plates were covered with tin foil to shield from light and place in a in water bath at 37°C for 30 minutes.
8. TRAP staining solution was aspirated, and all wells were washed 3 times with PBS.

Imaging and Quantification of Osteoclasts

Osteoclasts were identified as TRAP positive cells with three or more nuclei and a defined membrane. Osteoclast were visualized with bright field microscopy using the Olympus IX73 microscope. Osteoclast Images were recorded at 4X, 10x and 20x magnification. The whole well was visualized by taking multiple images at 4X magnification and used to count all osteoclasts.

RNA Isolation

At each time point a number of wells were assigned for total RNA extraction according to the following protocol:

1. The medium was aspirated and washed 2 times with 1ml PBS being careful to not contact the bottom of the well.
2. Trizol Reagent (300 ul) was added to each well for 5 minutes.
3. The pipette tip was used to scrape the bottom surface of the well to detach all cells and draw into pipette.
4. Samples were placed in 1.5ml Eppendorf tubes and stored in -20°C.
5. Chloroform (60 ul) per 300ul Trizol reagent were added to homogenize the sample.
6. The tubes were shaken by hand for 15 seconds and incubated for 2-3minutes at room temperature.
7. Samples were centrifuged at 12 000 x g for 15 minutes at 4°C.

(**NOTE:** The mixture separated into a lower red phenol-chloroform phase, an interphase, and a colorless upper aqueous phase. RNA was in the aqueous phase only.)

8. The aqueous phase was removed by angling the tube a 45° and pipetting the solution out.

(**NOTE:** do not touch the interface or the organic layer)

9. The aqueous phase was placed into Eppendorf tubes.
10. Isopropanol 100% (150 ul) was added to the aqueous phase per 300ul Trizol reagent used for homogenization.
11. Samples were incubated for 10 minutes at air room temperature.
12. Samples were centrifuged at 12 000 x g for 10 minutes at 4°C.
13. The supernatant was removed from the tube, leaving only the RNA pellet.
14. The RNA pellet was washed with 75% ethanol (300 ul) per 300ul Trizol reagent used for homogenization.
15. Each tube was vortexed briefly, then centrifuged at 7500 x g for 5 minutes at 4°C.
16. The wash (Ethanol) was aspirated and steps 14 and 15 were repeated for a second wash.
17. The wash (Ethanol) was aspirated. The RNA pellet was vacuum or air dried for 5-10 minutes.

(**NOTE:** Do not dry the RNA pellet by vacuum centrifuge and do not allow the RNA pellet to compete dry as the pellet may lose solubility.)

18. The RNA pellet was resuspended in 20ul of RNase free water
19. RNA concentration was estimated using a Nanodrop 1000 fiber optic spectrophotometer (Thermo Scientific) and stored at -80°C.

RNA reverse transcribed into cDNA

Total RNA derived from mice bone marrow was reversed transcribed into complementary deoxyribonucleic acid (cDNA) using the following protocol:

1. For each experimental condition, there were 2 wells assigned for RNA extraction. Therefore, we used 2.5 ul of RNA from each well for each experimental condition.
2. High-Capacity cDNA Reverse Transcription Kit (Applied Biosystems, Fisher Scientific) was used according to the manufacturer's recommended reaction composition:

- 10x RT Buffer: 2 ul
- 10x RT Random Primer: 2 ul
- dNTP Mix 100Mmol: 0.8 ul
- Multiscribe reverse transcriptase: 1 ul
- ddH2O: 9.2 ul

3. 15 ul of the cDNA reverse transcription mix was prepared for each experimental condition and 5 ul of total RNA for each experimental condition was added to this mix.
4. All samples were place in the Eppendorf Mastercycler machine for cDNA reverse transcription using the following settings:

- 25°C for 10 minutes
- 37°C for 120 minutes
- 85°C for 5 minutes
- 4°C for infinite hold

Quantitative Real Time PCR

Gene expression in osteoclast cultures was assessed by quantitative real-time PCR. Table 1 indicates the primer genes used with primer 36B4 serving as an internal control for normalization. Real time PCR amplification were performed using the SYBR Green Supermix (Bio-Rad). Reactions were carried out in Hard Shell 96 well PCR plates (Bio-Rad) with a total volume of 16 ul and included 8 ul of each primer and 8 ul of cDNA. The plates were covered Microseal B seal (Bio-Rad) and centrifuged at 500 g for 3 minutes. The plates were placed in a CFX96 Real-Time System (Bio-Rad) with the thermal cycler conditions as follows:

1. 95°C for 3 minutes
2. 95°C for 10 seconds
3. 60°C for 30 seconds
4. 95°C for 39 cycles
5. 60°C for 31 seconds
6. 60°C for 5 seconds
    a. +0.5°C /cycle
    b. Ramp 0.5°C /s
7. 60°C for 70 cycles
8. 4°C infinite hold

The specificities of the PCR amplifications were assessed by the examination of the melt curves to confirm the presence of single gene-specific peaks. The threshold cycle (Cq), defined as the cycle number at which the number of amplified gene of interest reached a fixed threshold, was set to 40 cycles. All measurements were performed in duplicates and analyzed using the $2^{-\Delta\Delta Cq}$ method[66].

Table 1: Primers used for Quantitative RT-PCR

Molecule	Sense primer Antisense primer	
36B4	5'-GTG TGT CTG CAG ATC GGG TA-3' 5'-CAG ATG GAT CAG CCA GGA AG-3'	
Chordin	5'-GCCATGACACTGGAGACCAA-3' 5'-ATCTGTCATAGCGGGCACTG-3'	NM_009893.2
BMP2	5'-TGA ATC AGA ACA CAA GTC AGT GGG-3' 5'-TGG AGC GGA TGT CCT TTT CC-3'	NM_007553
TRAP	5'-GAGTTGCCACACAGCATCAC-3' 5'-CGTCTCTGCACAGATTGCAT-3'	NM_007388
Calcitonin Receptor	5'-CCTGTTCACGAGAAGGAACC-3' 5'-GGGAGCAGGGCTACTACACA-3'	NM_007588
MMP9	5'-CTGTCGGCTGTGGTTCAGT-3' 5'-AGACGACATAGACGGCATCC-3'	NM_013599
Cathepsin K	5'-CACTGCTCTCTTCAGGGCTT-3' 5'-ACGGAGGCATTGACTCTGAA-3'	NM_007802
Twisted Gastrulation 1	5'-TGACGTTCCTGCTGTGTCTC-3' 5'-AGCATGCACTCCTTACAGCA-3'	NM_023053

Statistical Analysis

In-vitro analysis of BMP2, CHRD, TWSG1 during osteoclast differentiation

Osteoclast Quantification

Osteoclasts were identified as TRAP positive cells with three or more nuclei and a defined membrane. This experiment was repeated four times, therefore, n = 4. A one-way anova multiple comparison post-hoc statistical analysis was applied to assess significance level of osteoclast numbers between different time points (see Appendix).

Gene expression

Gene expression in osteoclast cultures was assessed by quantitative real-time PCR. A series of t-tests were done to determine if a significant difference exists between the mean expression levels of the genes analyzed (see Appendix). The genes analyzed were: BMP2, TWSG1, CHRD,

MMP9, CTR, TRAP, and CTSK. The mean gene expression at day 4 induction (MCSF + RANKL) was compared to day 2 uninduced (MCSF only) which served as the control.

In-vitro analysis to determine whether CHRD directly controls osteoclast differentiation

Osteoclast Quantification

Osteoclasts were identified as TRAP positive cells with three or more nuclei and a defined membrane. This experiment was repeated four times, therefore, n = 3. The statistical test used were t-tests to determine if a significant difference exists between the means of osteoclast numbers in different conditions (see Appendix). The mean number of osteoclasts in WT LD condition was compared to CHRD LD and similarly WT HD compared to CHRD HD.

Gene expression

Gene expression in osteoclast cultures was assessed by quantitative real-time PCR. A series of t-tests were done to determine if a significant difference exists between the mean expression levels of the genes analyzed (see Appendix). The genes analyzed were: MMP9, CTR, TRAP, and CTSK. The mean gene expression at day 8 induction (MCSF + RANKL) from the CHRD KO culture was compared to day 8 induced from the WT culture. This was done for all genes in both the LD and HD conditions.

Chapter 4: Results

In-vitro analysis of BMP2, CHRD, TWSG1 during osteoclast differentiation

It was previously reported that BMP2 and TWSG1 are expressed during osteoclast differentiation[50]. However, there has been no studies looking at the expression of CHRD during osteoclast differentiation. Dr. Graf's preliminary results from the ligature model in mice indicated that CHRD expression is associated with the formation of clastic cells (Fig. 14 in introduction)[51]. We thus wanted to establish if and when CHRD is expressed during osteoclast differentiation.

In order to do this, we first had to establish an in-vitro osteoclast differentiation protocol (outlined in Chapter 3). Bone marrow cells from WT mice were cultured and induced with either M-CSF (control) or M-CSF and RANKL (induced) for osteoclast differentiation. The TRAP staining protocol was used at different time points to visualize osteoclasts. We extracted cell samples at different time point for RNA extraction, which was transcribed to cDNA and used to assess gene expression using RT-qPCR.

The TRAP staining protocol yielded TRAP positive cells when the cultured bone marrow cells were induced with M-CSF and RANKL. We can appreciate the progressive change of TRAP positive cells from day 2 to day 8. At Day 4, we observed multiple large cells, which stained positive but did not form syncytia. At day 6 and 8 there were numerous TRAP positive cells. In contrast, the control cells which were induced with only M-CSF were visible as TRAP negative cells (Fig. 1). At a higher magnification, we can appreciate that the TRAP positive cells contain multiple nuclei indicative of mature osteoclasts (Fig. 2). Note, it is a standard feature of osteoclasts cultures that although all cells are being induced to differentiate, only a small percentage of cells will actually form syncytia, an indication of mature osteoclasts.

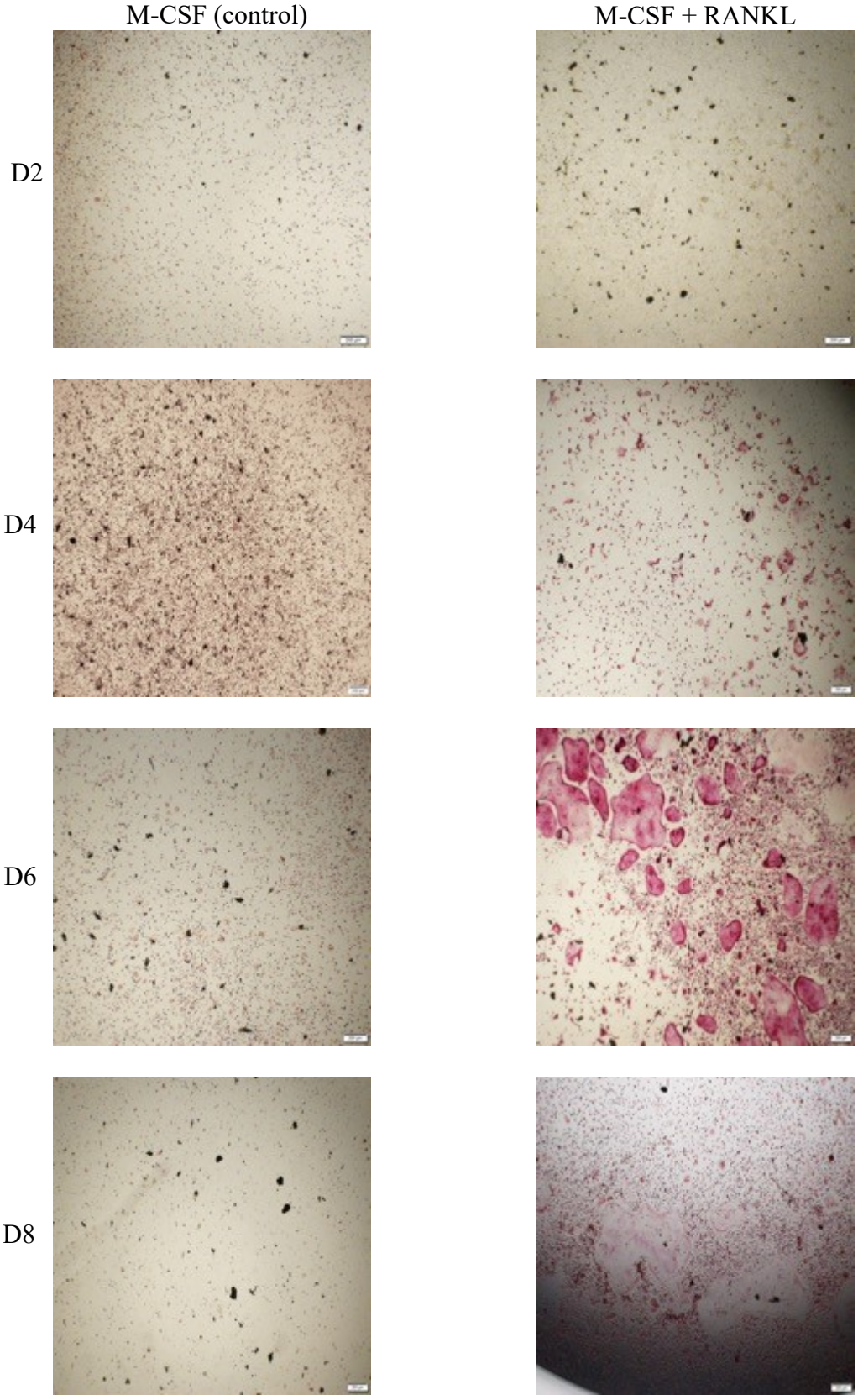
M-CSF (control)
M-CSF + RANKL
D2
D4
D6
D8

Figure 1: Bright field microscopy at 4X magnification showed control cells at each time point were visible as TRAP negative cells, while induction with M-CSF and RANKL led to the formation of TRAP-positive syncytia (multinucleated cells) indicative of mature osteoclasts. At day 6 and 8, there was a marked increase in the formation of TRAP-positive cells. Scale bar = 200um, Representative of n = 4.

(a)

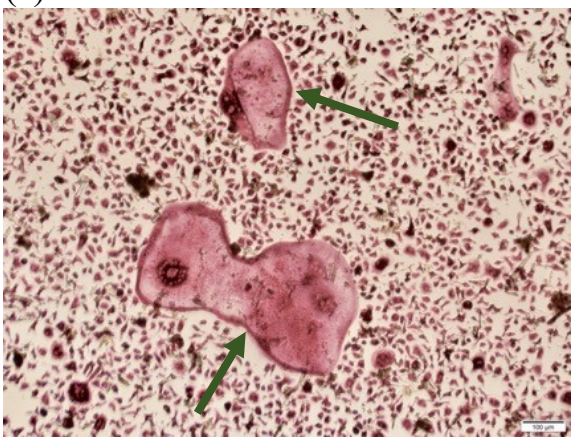

(b)

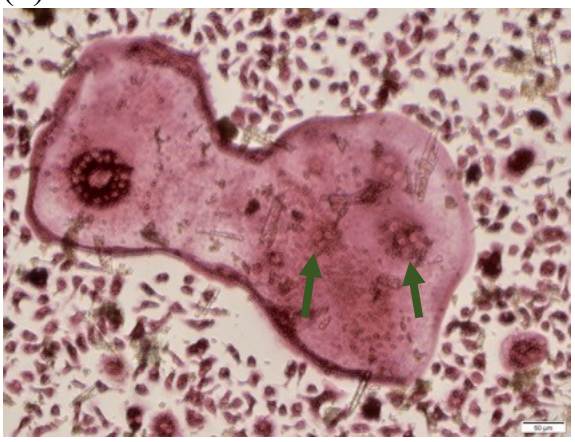

Figure 2: (A) Bright field microscopy at 10X magnification demonstrates multiple large, multinucleated osteoclasts depicted by the green arrows. Scale bar = 100um (B) Bright field micrograph at 20X magnification demonstrates a multinucleated TRAP positive osteoclast. There are numerous round structures within the osteoclast indicative of nuclei, an example of which is shown by the green arrows. Scale bar = 50um.

An osteoclast was defined as being a TRAP positive cell with ≥3 nuclei and a defined membrane. This allowed the number of osteoclasts to be quantified at each time point (Table 1, Fig. 3). This experiment was repeated four times. At day 2, there was no osteoclasts present and at day 4 only a few osteoclasts were expressed. It was at day 6 that we saw a significant increase in the number of osteoclasts. However, at day 8 there was a decrease in the mean number of osteoclasts which still proved to be higher than day 2 and day 4.

	Day 2	Day 4	Day 6	Day 8
Experiment 1	0	1	51	17
Experiment 2	0	3	73	21
Experiment 3	0	2	64	12
Experiment 4	0	5	97	16
Mean	0	2.75	71.25	16.5

Table 1: Osteoclast quantification. Number of osteoclasts were recorded at each time point each time the experiment was repeated. The mean number of osteoclasts were calculated. n= 4.

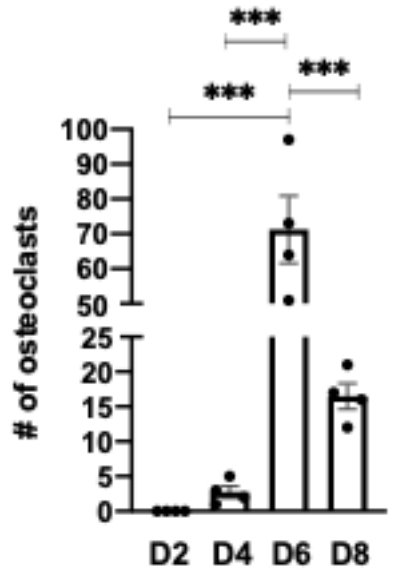

Figure 3: Osteoclast quantification. The bars represent the mean number of osteoclasts at each time point each time the experiment was repeated. Each black dot at each time point represents the number of osteoclasts recorded at each experiment. n= 4, $p < 0.001$.

The samples collected for RNA extraction at 2, 4, 6, 8 days following M-CSF or M-CSF and RANKL induction were analyzed for various gene expression by RT-qPCR. The genes included: 36B4 (house-keeping gene), BMP2, TWSG1, CHRD, MMP9, CTR, TRAP, and CTSK. The graphs in figure 4 represent the mean expression for each gene at each time point.

The results showed that the expression of BMP2 gradually increased from day 2 and peaked at day 6. A similar pattern of expression was seen for BMP2 antagonists: TWSG1 and CHRD. TWSG1 and CHRD both had a peak expression at day 4. The expression of BMP2 decreased at day 8 which was comparable to its day 2 expression. This decrease in expression was mirrored in BMP2 antagonists, TWSG1 and CHRD (Fig. 4). There was a strong expression of osteoclast specific genes: MMP9, CTR, TRAP, and CTSK. In particular, MMP9, CTR, and TRAP had a strong expression at day 4 which was followed by a gradual decrease at day 6 and 8. Meanwhile, the expression of CTSK gradually increased until day 6 which was followed by a decrease in expression at day 8. The enhanced expression of these osteoclast-specific markers was indicative of successful osteoclast differentiation. However, the patterns of gene expression seen were not statistically significant. The samples collected from the control cells had negligible expression of the tested genes.

For most genes, the strongest expression was observed at day 4 RANKL. Therefore, day 4 was selected as the reference to which other days were compared. The gene expression at day 4 RANKL was set to 1 and used as the reference to which other days were compared (Fig. 5). This experiment was repeated four times and as such an average gene expression was calculated.

The results showed that the average relative gene expression of BMP2 peaked at day 4 with a gradual decrease at day 6 and 8. A similar pattern of expression was seen for BMP2 antagonists:

TWSG1 and CHRD. With respect to osteoclast specific genes, the average relative gene expression gradually increased at day 6 and 8 except MMP9 which showed a decrease in gene expression at days 6 and 8 relative to day 4.

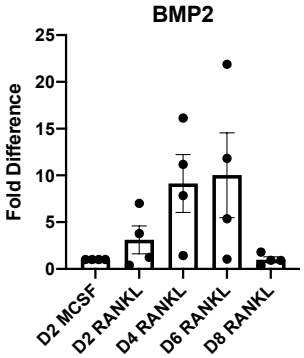
BMP2
Fold Difference
25
20
15
10
5
0
D2 MCSF
D2 RANKL
D4 RANKL
D6 RANKL
D8 RANKL

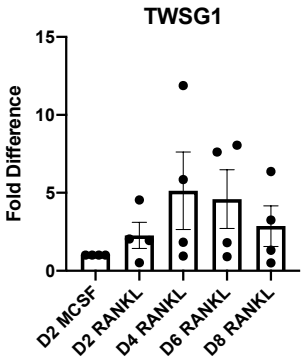
TWSG1
Fold Difference
15
10
5
0
D2 MCSF
D2 RANKL
D4 RANKL
D6 RANKL
D8 RANKL

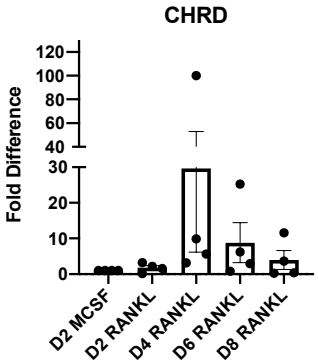
CHRD
Fold Difference
120
100
80
60
40
30
20
10
0
D2 MCSF
D2 RANKL
D4 RANKL
D6 RANKL
D8 RANKL

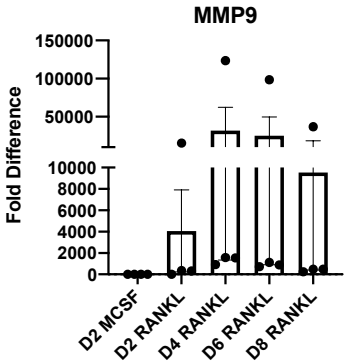
MMP9
Fold Difference
150000
100000
50000
10000
8000
6000
4000
2000
0
D2 MCSF
D2 RANKL
D4 RANKL
D6 RANKL
D8 RANKL

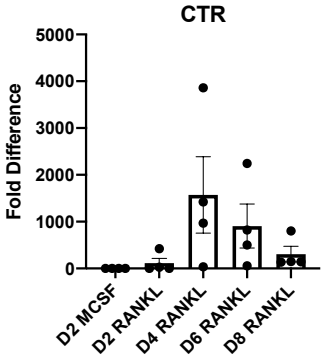
CTR
Fold Difference
5000
4000
3000
2000
1000
0
D2 MCSF
D2 RANKL
D4 RANKL
D6 RANKL
D8 RANKL

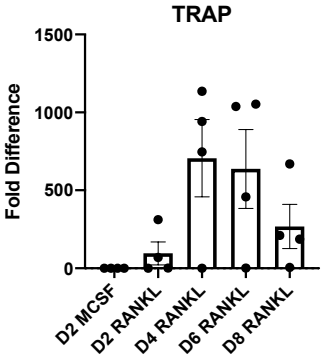
TRAP
Fold Difference
1500
1000
500
0
D2 MCSF
D2 RANKL
D4 RANKL
D6 RANKL
D8 RANKL

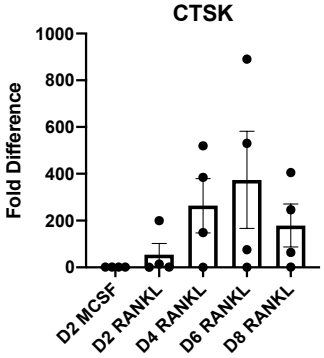
CTSK
Fold Difference
1000
800
600
400
200
0
D2 MCSF
D2 RANKL
D4 RANKL
D6 RANKL
D8 RANKL

Figure 4: Osteoclast cultures at 2-, 4-, 6-, and 8-days after induction with M-CSF (control) or M-CSF and RANKL (induced) were analyzed using RT-qPCR for the following genes: 36B4 (housekeeping), BMP2, TWSG1, CHRD, MMP9, CTR, TRAP, CTSK.

BMP2 had a peak expression at day 4 along with its antagonists: TWSG1 and CHRD. There was a strong expression of osteoclast specific markers: MMP9, CTR, TRAP, and CTSK. No CHRD expression was detected in control cells. n= 4.

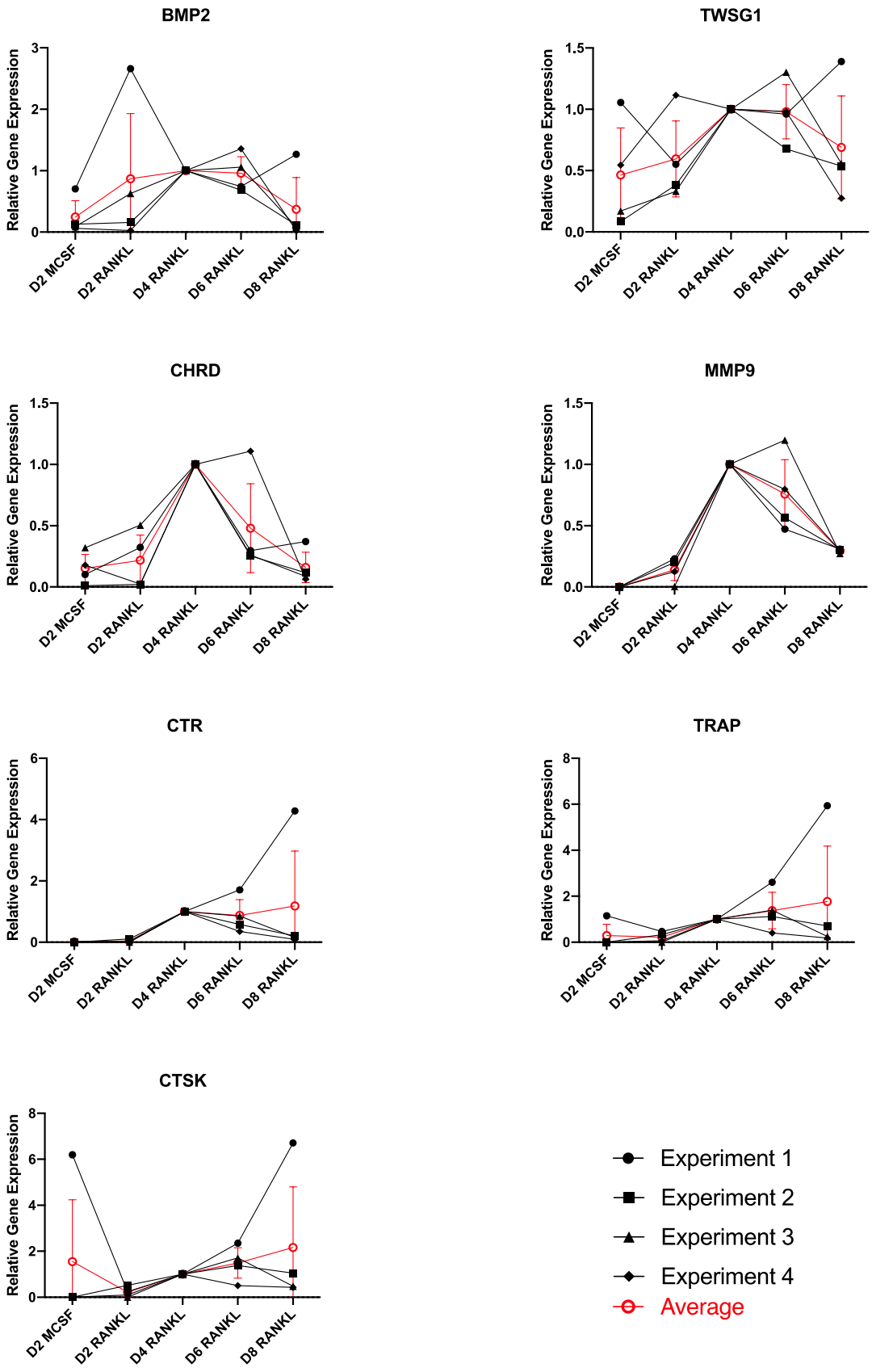
BMP2
TWSG1
CHRD
MMP9
CTR
TRAP
CTSK
Relative Gene Expression
D2 MCSF
D2 RANKL
D4 RANKL
D6 RANKL
D8 RANKL
Experiment 1
Experiment 2
Experiment 3
Experiment 4
Average

Figure 5: Relative gene expression following osteoclast induction. Gene expression at day 4 RANKL was set to 1 and used as the reference to which other days were compared.
the gene expression for the other days were calculated relative to day 4. BMP2 peaked at day 4 with a gradual decrease at day 6 and 8. A similar pattern was seen for TWSG1 and CHRD. Osteoclast specific genes had a gradual increase from day 2 to day 8 expect MMP9. n = 4.

In-vitro analysis to determine whether CHRD directly controls osteoclast differentiation

Having established that CHRD, BMP2, and TWSG1 are dynamically expressed during osteoclast differentiation, we set up to determine the potential role of CHRD in osteoclast differentiation. In order to do this, bone marrow cells from WT control and CHRD-KO mice were cultured in low density (LD) or high density (HD) conditions and induced with either M-CSF (control) or M-CSF and RANKL (induced) for osteoclast differentiation. The TRAP staining protocol was used at different time points to visualize osteoclasts. We extracted cell samples at different time point for RNA extraction, which was transcribed to cDNA and used to assess gene expression using RT-qPCR.

The TRAP staining protocol yielded TRAP positive cells when the cultured bone marrow cells from the WT and CHRD-KO mice in both low density (LD) and high density (HD) conditions were induced with M-CSF and RANKL. We can appreciate the progressive change of TRAP positive cells from day 4 to day 8 in all conditions (Fig. 6, 7). In particular, at day 8 there were numerous TRAP positive cells. In contrast, the control cells which were induced with only M-CSF were visible as TRAP negative cells. Although at day 4 induction with M-CSF and RANKL led to the formation of TRAP-positive syncytia, multinucleated cells indicative of mature

osteoclasts could not be detected. However, at day 8 there were numerous TRAP positive cells containing multiple nuclei indicative of mature osteoclasts (Fig. 8).

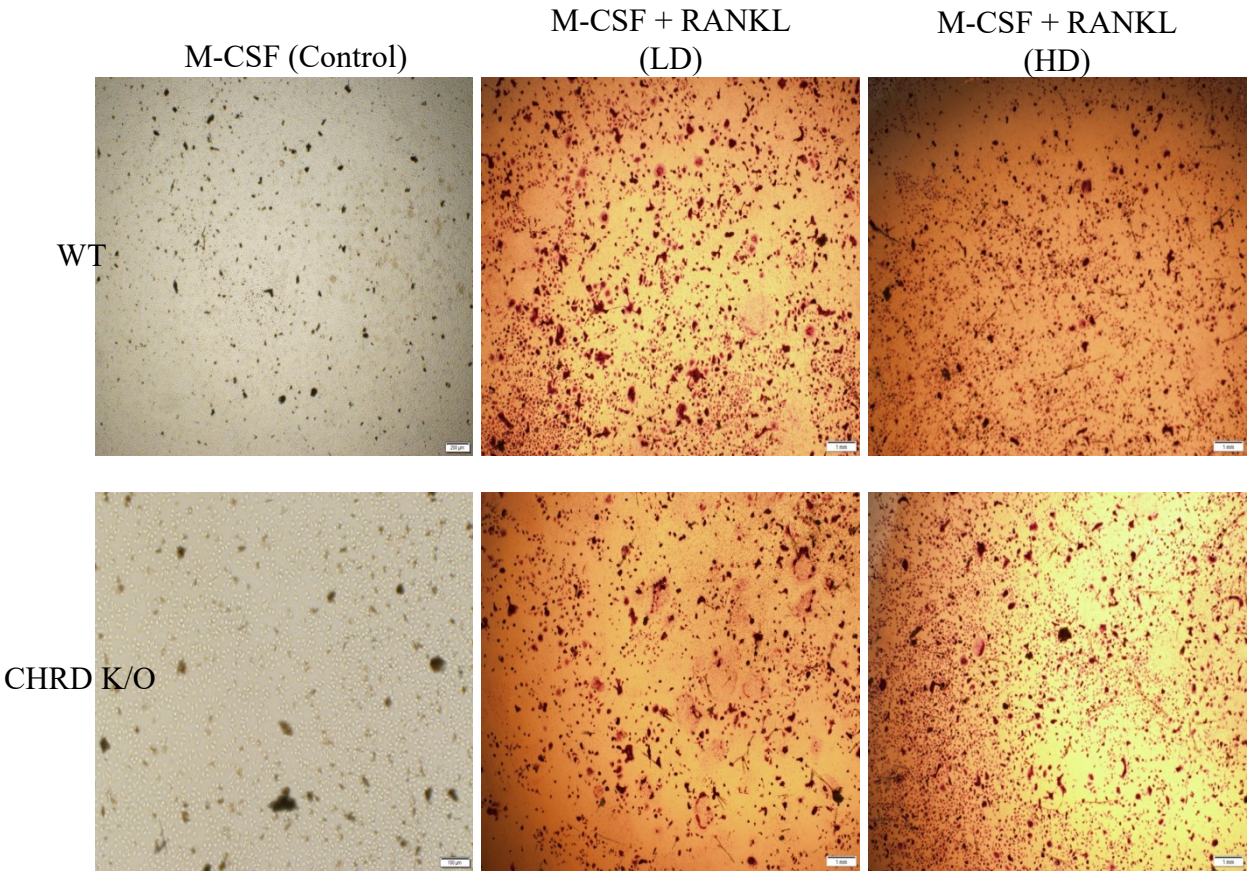

Figure 6: TRAP staining of cultured bone marrow cells from a WT and a CHRD-KO mice at day 4 induction with M-CSF (control) or M-CSF and RANKL (induced). The bone marrow cells were cultured either in low density (LD) or high density (HD). Bright field microscopy at 10X magnification showed control cells were visible as TRAP negative cells. Although, induction with M-CSF and RANKL led to the formation of TRAP-positive syncytia, multinucleated cells indicative of mature osteoclasts could not be seen. Scale bar = 1mm, n = 3.

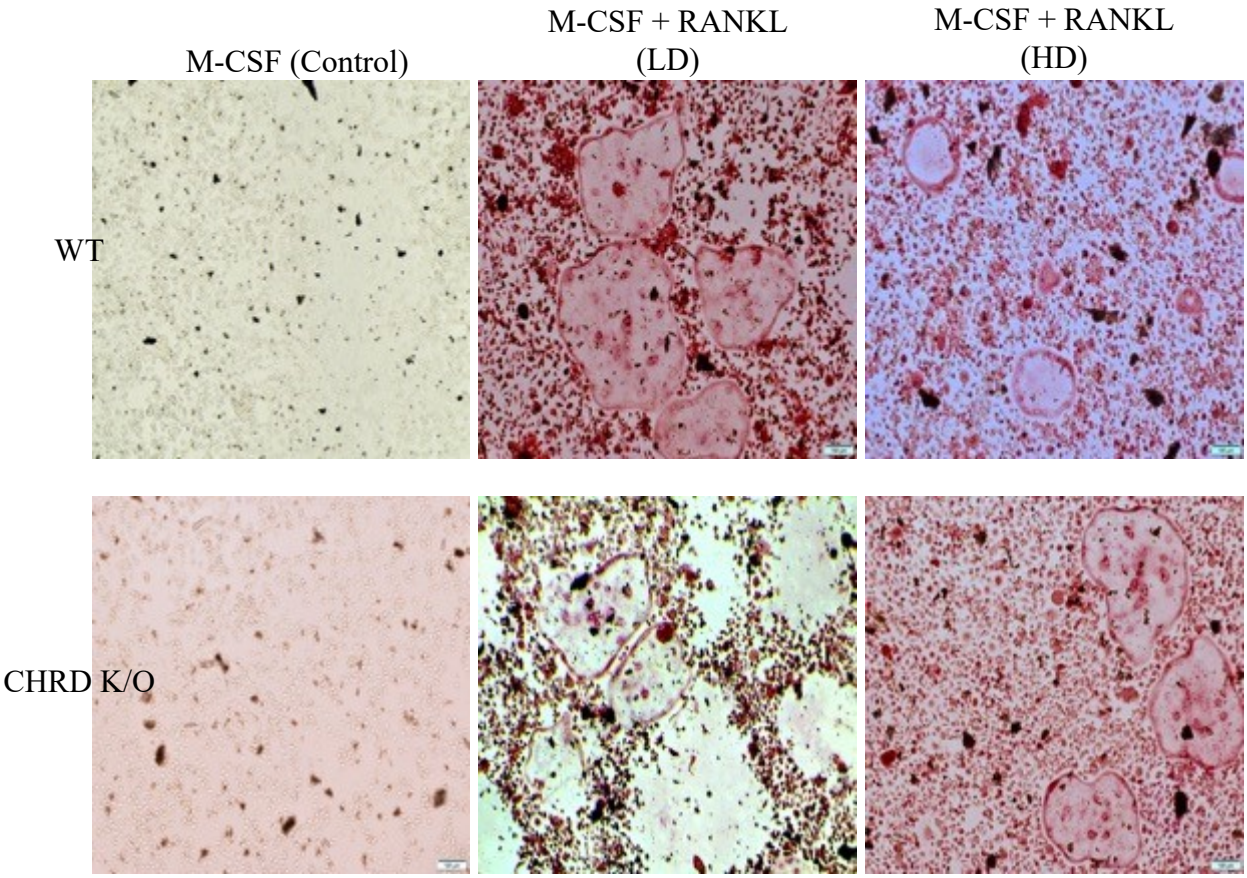

Figure 7: TRAP staining of cultured bone marrow cells from a WT and a CHRD-KO mice at day 8 induction with M-CSF (control) or M-CSF and RANKL (induced). The bone marrow cells were cultured either in LD or HD. Bright field microscopy at 10X magnification showed control cells at each time point were visible as TRAP negative cells, while induction with M-CSF and RANKL led to the formation of TRAP-positive syncytia (multinucleated cells) indicative of mature osteoclasts. Scale bar = 100um, n = 3.

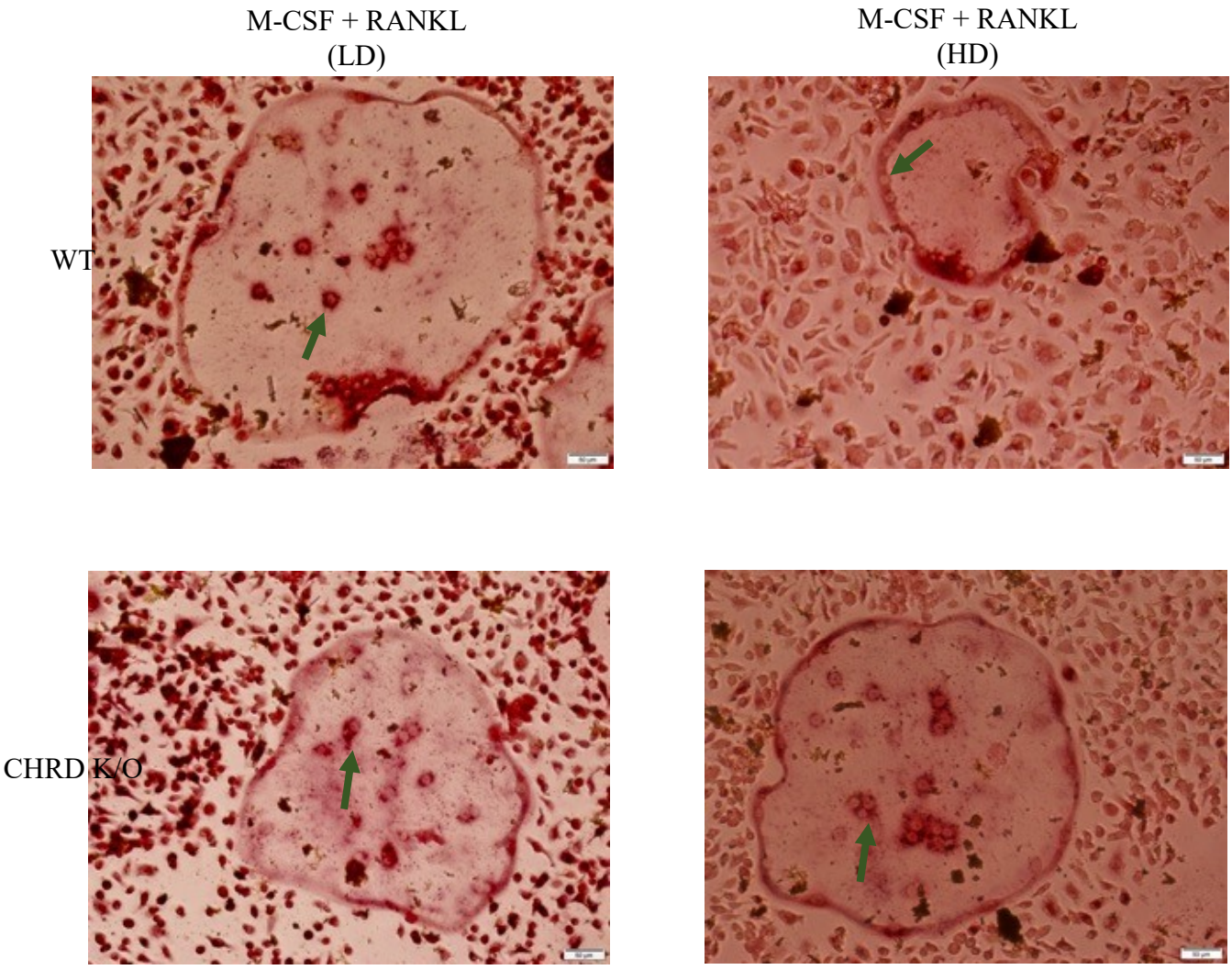

Figure 8: Bright field microscopy at 20X magnification demonstrates large, multinucleated TRAP positive osteoclasts in WT and CHRD-KO mice when induced with M-CSF and RANKL in both LD and HD cell cultures. There are numerous round structures within the osteoclast indicative of nuclei, an example of which is shown by the green arrows. Scale bar = 50um.

An osteoclast was defined as being a TRAP positive cell with ≥3 nuclei and a defined membrane. This allowed the number of osteoclasts to be quantified at each time point. This experiment was repeated three times. At day 4, there was no osteoclasts present in any of the tested conditions. However, at day 8, there was an increase in the number of osteoclasts in all the tested conditions (Table 2, Fig. 8). Particularly, there were more osteoclasts present in the low-density LD) wells compared to the high-density wells (HD) in both the wild type (WT) and Chordin knockout (CHRD KO) mice. However, comparing the number of osteoclasts generated in WT LD with CHRD KO LD proved to be not significant ($p = 0.483$). Similarly, comparing osteoclast numbers in WT HD with CHRD KO HD proved to be not significant ($p = 0.904$).

	WT LD	WT HD	CHRD K/O LD	CHRD K/O HD
Experiment 1	18	24	22	21
Experiment 2	21	14	4	9
Experiment 3	70	16	43	22
Mean	36.33	18.00	23.00	17.33

Table 2: Osteoclast quantification. Number of osteoclasts were recorded at day 8 for each condition. The mean number of osteoclasts were calculated. n= 3.

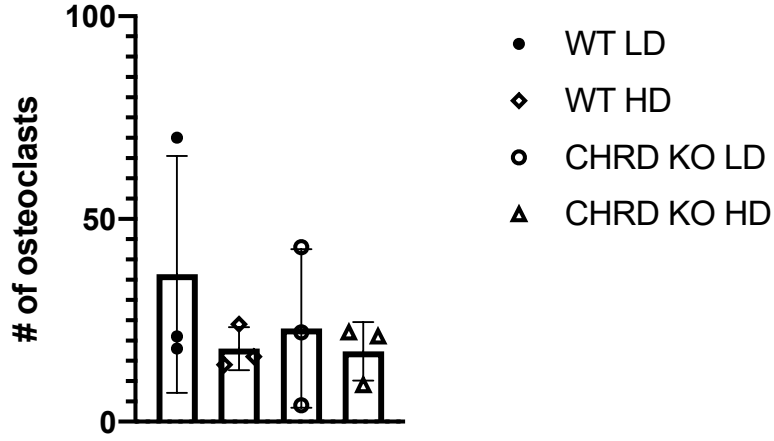

Figure 9: Osteoclast quantification. The bars represent the mean number of osteoclasts for each condition. Each symbol for each condition represents the number of osteoclasts recorded at each experiment. n= 3.

The cell samples collected for RNA extraction in low density (LD) or high density (HD) at 4- and 8-days following M-CSF and RANKL induction were analyzed for osteoclast specific gene expression by RT-qPCR. The genes included: 36B4 (house-keeping gene), MMP9, CTR, TRAP, and CTSK. The gene expression at day 4 M-CSF was set to 1 and used as the reference to which other days and conditions were compared. This experiment was repeated three times and as such an average gene expression was calculated. A significantly stronger expression of osteoclast-specific genes was seen in CHRD-deficient cells in comparison to the WT cells under all conditions tested (high or low density, after 4 and 8 days of differentiation) (Fig. 10). However, the exceptions were from the WT control in the LD osteoclast cultures at day 4 which had a higher expression of MMP9 compared to CHRD KO cultures. A similar expression was seen for CTR in the HD osteoclast cultures. The patterns of gene expression seen were not statistically significant.

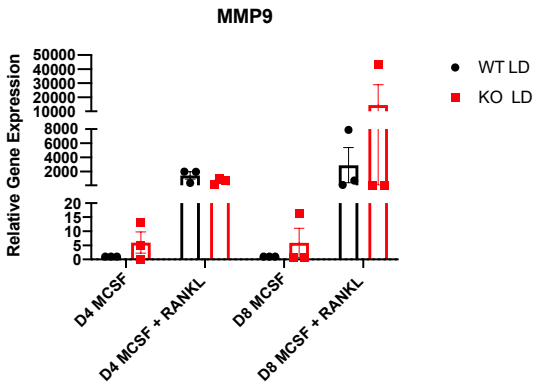
MMP9
Relative Gene Expression
50000
40000
30000
20000
10000
8000
6000
4000
2000
20
15
10
5
0
D4 MCSF
D4 MCSF + RANKL
D8 MCSF
D8 MCSF + RANKL
WT LD
KO LD

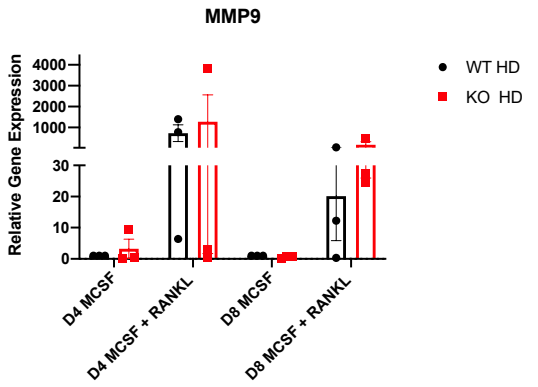
MMP9
Relative Gene Expression
4000
3000
2000
1000
30
20
10
0
D4 MCSF
D4 MCSF + RANKL
D8 MCSF
D8 MCSF + RANKL
WT HD
KO HD

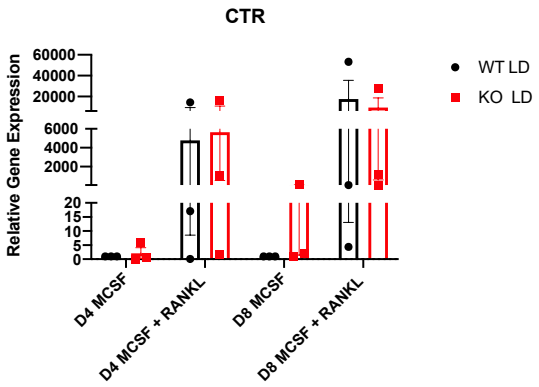
CTR
Relative Gene Expression
60000
40000
20000
6000
4000
2000
20
15
10
5
0
D4 MCSF
D4 MCSF + RANKL
D8 MCSF
D8 MCSF + RANKL
WT LD
KO LD

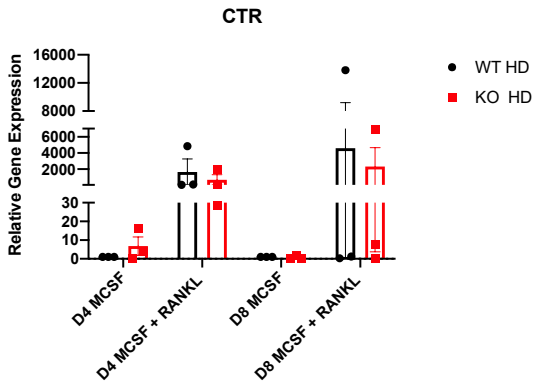
CTR
Relative Gene Expression
16000
12000
8000
6000
4000
2000
30
20
10
0
D4 MCSF
D4 MCSF + RANKL
D8 MCSF
D8 MCSF + RANKL
WT HD
KO HD

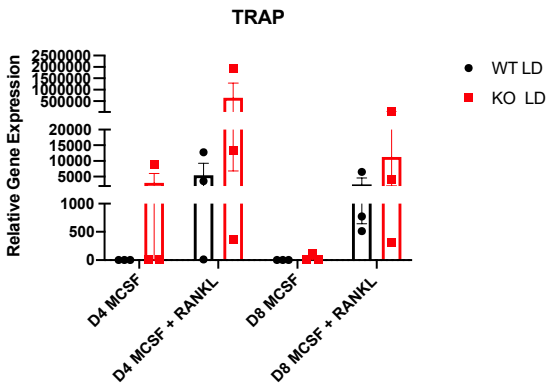
TRAP
Relative Gene Expression
2500000
2000000
1500000
1000000
500000
20000
15000
10000
5000
1000
500
0
D4 MCSF
D4 MCSF + RANKL
D8 MCSF
D8 MCSF + RANKL
WT LD
KO LD

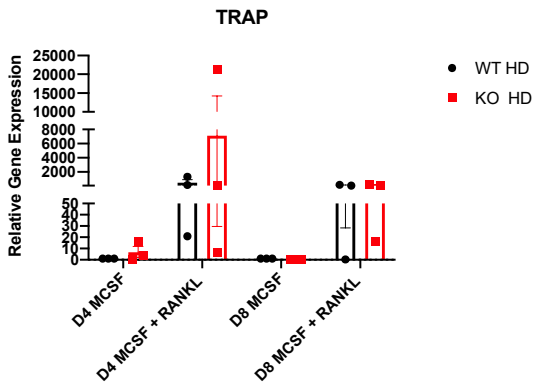
TRAP
Relative Gene Expression
25000
20000
15000
10000
8000
6000
4000
2000
50
40
30
20
10
0
D4 MCSF
D4 MCSF + RANKL
D8 MCSF
D8 MCSF + RANKL
WT HD
KO HD

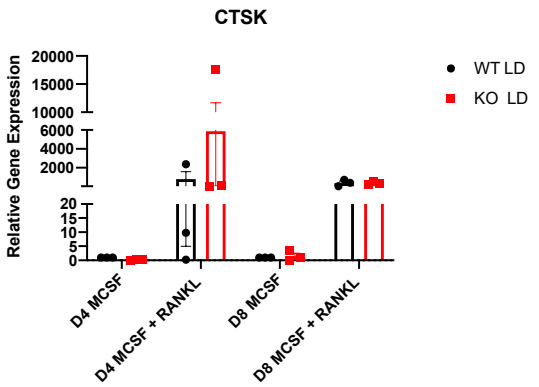
CTSK
Relative Gene Expression
20000
15000
10000
6000
4000
2000
20
15
10
5
0
D4 MCSF
D4 MCSF + RANKL
D8 MCSF
D8 MCSF + RANKL
WT LD
KO LD

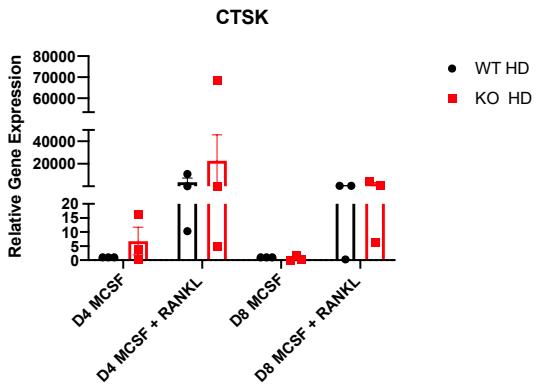
CTSK
Relative Gene Expression
80000
70000
60000
40000
20000
20
15
10
5
0
D4 MCSF
D4 MCSF + RANKL
D8 MCSF
D8 MCSF + RANKL
WT HD
KO HD

Figure 10: Relative gene expression of osteoclast cultures in low density (LD) or high density (HD) at 4- and 8-days after induction with RANKL were analyzed using RT-qPCR for the following genes: MMP9, CTR, TRAP, and CTSK. Gene expression at day 4 M-CSF was set to 1 and used as a reference to which other days and conditions were compared. n= 3.

Chapter 5: Discussion

Our study aimed to identify how BMP2 and CHRD regulate the in-vitro differentiation of osteoclasts from mouse bone marrow precursor cells of C57Bl6 and CHRD KO mice. The study boasted many strengths, some which include: (a) use of primary cells extracted from the bone marrow; (b) use of a novel CHRD KO mice; (c) Each experiment was repeated 3 or 4 times using independent cultures; (d) monitoring and quantifying the number of osteoclasts cytochemically in each experiment; and (e) quantifying and comparing different marker genes during osteoclastogenesis by RT-qPCR.

Before we set out to explore the interaction of BMP2 and CHRD in osteoclastogenesis, we established an osteoclast differentiation protocol for bone marrow cells derived from WT and CHRD KO mice. We then performed a quantitative analysis of osteoclast numbers using TRAP staining and gene expression using RT-qPCR.

In the time course experiment, we compared the number of osteoclasts generated from C57Bl6 bone marrow precursors plated at a density of 2 $x10^5$ cells per 48 well plate and induced with M-CSF (30 ng/ml) and RANKL (50 ng/ml) at different time points. Previous studies have established the critical role of M-CSF in inducing clonal expansion of bone marrow derived osteoclast precursor cells and the up-regulation of RANK allowing these cells to interact with RANKL and differentiating into osteoclasts[67-69]. Previous research has also highlighted the role of RANK and RANKL in osteoclast formation. Most notably these studies have shown that in mice with deficient RANK/RANKL expression osteopetrosis ensues due to the lack of osteoclast production, a process which is critical in the bone remodeling process[27-29].

We observed that well-formed osteoclasts were visible by day 4, reaching a peak number by day 6, and a decline day 8, status post RANKL induction (Fig. 3 in results). In contrast, the control cells which were induced with only M-CSF yielded no osteoclasts. Although we noted a significant number of osteoclasts in the induced cell culture, there were many stromal cells that did not differentiate into mature osteoclasts. This may be best explained by the interaction between osteoclast precursor cells and other stromal cells present in the culture, which ultimately affects the dynamics of osteoclast precursor cells and osteoclastogenesis. To maximize the number of osteoclasts we induced the precursor cells with 50 ng/ml RANKL and changed the medium every other day. This was in accordance with the protocols followed by another study by Boraschi-Diaz where osteoclastogenesis was not affected by RANKL above 50 ng/ml and a similar osteoclast yield was achieved. Therefore, we concluded that optimal conditions for osteoclastogenesis from mouse bone marrow cells required cell plating at 2 $x10^5$ cells per 48 well plate, induction with M-CSF (30 ng/ml) and RANKL (50 ng/ml) for 6 days with a complete medium change every 48 hours. In this experiment, we successfully created the conditions for in-vitro osteoclast differentiation, however, a different set of conditions are required in order to isolate these osteoclasts to assess their functionality. Osteoclasts require a substantial amount of energy to enable their motility and specialized functions related to bone resorption. One important energy source is glucose, and its suppression is linked to decreased osteoclast function. In addition, studies have shown that both glycolysis and the Kerbs cycle are vitals sources of energy for osteoclast formation and function[70, 71]. Therefore, in subsequent studies we can create these conditions to isolate osteoclasts on dentin discs and assess their functionality by quantifying their resorptive capabilities.

Next, we examined the expression of various genes at different time points using RT-qPCR. The osteoclasts showed a robust expression of TRAP, CTSK, MMP9, and CTR which was in accordance with findings of other studies[72, 73]. The up regulation of TRAP, CTSK, MMPs was a sign of osteoclastogenesis as these degradative enzymes have been established for their role in bone resorption. On the other hand, CTR is highly expressed on mature osteoclasts allowing it to interact with calcitonin which subsequently inhibits osteoclastic bone resorption. Despite the role CTR plays in bone resorption inhibition, when all these four signals are expressed together, they induce a homoeostatic balance which ultimately results in optimal conditions for bone production. Our findings showed that osteoclast specific markers were expressed in the induced precursor cells at all time points. In particular, the average relative gene expression of TRAP, CTSK, and CTR gradually increased on days 6 and 8 except MMP9 which showed a decrease in gene expression on days 6 and 8 relative to day 4 (Fig. 5 in results). Takeshita et al. reported that mRNA expression levels of TRAP and CTSK were elevated as early as day 2, while on day 4 there was a strong expression of TRAP, CSTK, MMP9, and CTR[73]. In another study, a strong expression of CTR, CTSK, and MMP9 was seen on day 5 in osteoclasts generated from bone marrow precursors[72]. Therefore, we can conclude from our findings and previous studies that transcriptional up-regulation of osteoclast specific markers occurs during early stages of differentiation in pre-osteoclasts which are cells committed to the osteoclast lineage[67, 73].

A novel aspect of this experiment was examining the potential interaction of BMP2 and its antagonist during osteoclastogenesis by assessing their expression kinetics. The results showed that the average relative gene expression of BMP2 on days 6 and 8 had a gradual decline when compared to its peak expression on the fourth day. A similar pattern of expression was seen for

BMP2 antagonists: TWSG1 and CHRD. Literature currently has established that in the presence of RANKL, BMP2 enhances in-vitro osteoclastogenesis of bone marrow cells[47]. TWSG1 deficient mice showed a greater expression of osteoclasts when compared to WT mice while the overexpression of TWSG1 decreased the size and number of osteoclasts. Interestingly, when these cells were induced with exogenous BMP2 osteoclastogenesis was restored[50] confirming the opposing activities of BMP2 and TWSG1 on osteoclasts. With regards to CHRD, there is evidence to support its selective inhibition of BMP-2,-4, and-7, however, their role in osteoclastogenesis is poorly understood. Our findings demonstrated an interesting simultaneous increase in expression of CHRD with BMP2 and TWSG1 at day 4 and a simultaneous decrease on the following days. Despite the observed co-expression, it remains unclear whether or not CHRD interacts with BMP2 and TWSG1 in this system.

BMP2 has been demonstrated to play important roles in regulating the differentiation and function of osteoblasts and osteoclasts. It has been linked to major signalling pathway and biological processes that play a role in regulating bone cell energy metabolism. Genetic mutations of BMP2 signaling cause a wide variety of inheritable bone diseases in humans. For these reasons, further studies are needed to understand its specific role, associations and its mechanism of action. While our study did find a positive association between CHRD with BMP and TWSG, past literature does not support this finding. This could be due to the fact that other unknown confounding signals might influence these interactions which need to be explored. Also, the experimental conditions and methodologies vary significantly between studies leading to different and sometimes conflicting results.

In a study by Graf et al., a signalling network involving BMP2/CHRD/TWSG1 was explored where BMP-2/4 inhibits the development of thymocytes[65]. When thymocytes received a signal via pre-TCR (T-cell receptor), they secreted TWSG1 and together with CHRD removed the inhibitory action of BMP-2 resulting in thymocyte maturation.

Studies on Zebrafish has shown that TWSG1 can have an agonistic or an antagonistic effect on BMP signalling depending on the relative levels of Chordin/Sog (short gastrulation), TWSG1, and tolloids. When Chordin/Sog are cleaved by Tolloids, BMP signalling is reactivated possibly because TSWG1 binds to Chordin and prevents its inhibitory function on BMP signalling[74, 75]. Tolloids are metalloproteases with proteolytic activity specific for Chordin.

Although a signalling network involving BMP2/CHRD/TWSG1 has been established in thymocyte development and zebrafish development, further investigation is required to determine if a similar signalling network exists in osteoclast differentiation. If future investigations substantiate the mechanism of this network, it will build on our current body of knowledge with regards to the well-established RANK/RANKL/OPG system.

Based on our findings in time course experiments, we established that CHRD was dynamically expressed along with BMP2 and TWSG1. Therefore, we set out to explore whether CHRD has a direct effect on osteoclasts differentiation. To do this, we implemented the same protocol used in the time course experiment to compare osteoclast numbers and quantitative gene expression in CHRD deficient mice to WT control mice. To examine the effect of plating density of

osteoclastogenesis we plated the bone marrow cells in low density (2 x10^5 cells per 48 well plate) and high density (4 x10^5 cells per 48 well plate).

The results revealed successful osteoclast generation at day 8 in all the tested conditions, particularly in low-density wells compared to the high-density wells in both the WT and CHRD KO mice. In the study by Boraschi-Diaz, they examined the effect of plating density on osteoclastogenesis. Bone marrow cells from C57Bl6 mice were plated in 25, 50, or 100 x 10^3 cells/cm^2. They found that more osteoclasts were generated as plating density increased suggesting that osteoclastogenesis and plating density are directly proportional[72]. This was in conflict with our findings because we observed more osteoclasts in the low-density condition. This could be explained by the fact that in the Boraschi-Diaz study they used 6-17 weeks old mice, conditioned the precursor cells with 50 ng/ml M-CSF, and the experiment lasted only 5 days with a medium change on the 3rd and 5th day. In our study, we used 8-month-old mice, conditioned the precursor cells with 30 ng/ml M-CSF and allowed the experiment to run for 8 days. These distinct differences in experimental methodology may explain the conflicting results. In another study, most TRAP positive cells were seen at 5 x 10^3 cells per 96 well plate while higher plating densities had progressively fewer TRAP positive cells[76]. Although, a direct comparison between our study and others is not feasible due to different methodologies, we can reasonably conclude that plating density is a crucial determinant of osteoclastogenesis.
Based on the RT-qPCR results, the induced precursor cells from the WT and CHRD KO mice expressed more osteoclast specific markers under both low-density and high-density conditions (Fig 10 in results). However, this relationship does not appear to be significant and further studies are needed to establish solid and reproducible results. In order to have a better

understanding of these findings, it is important to consider that CHRD is not absolutely required for osteoclast formation. It is possible that there might be differential effects of lack of CHRD on expression levels of the various genes analyzed. For example, plating at low density showed a trend for increased CTSK and TRAP expression in CHRD mutant mice. However, further studies are required to determine its statistical significance. In addition, studies on resorption assays on dentin discs and quantification of resorption could help to gain a deeper understanding of the role of CTSK in relation to osteoclasts and matrix degradation. MicroCT analysis of bone parameters is another future step that could help build a more complete picture of these pathways, their relationships and the way in which they could transform future therapies.

Limitations:

There are a number of limitations to our study. Since our study included in-vitro experiments we cannot extrapolate our results to the biology of an intact organism. Furthermore, despite efforts to follow evidence-based protocols, it is not always possible to reproduce studies mainly due to their scope and objectives. While our study did show some associations in possible signalling pathways, there could still be signalling mechanism that we did not discover or entirely understand. This opens up the possibility to cofounding factors that were possibly unaccounted for. Due to the limited number of trials in our experiment, the principle of normalcy could not be established. This exposes the study to external bias. Finally, it is important to build a better understanding of Chordin knock out mice and their phenotypes before utilizing them in future studies, aiming to establish more significant results.

Future directions:

From the first set of experiments, we established that BMP2, TWSG1, and CHRD were dynamically expressed during osteoclast differentiation. A future experiment should characterize how the interaction of BMP2, TSWG1, and CHRD effects osteoclastogenesis in-vitro with a more detailed look at their mechanism. This could potentially be accomplished by harvesting bone marrow cells from C57Bl6 mice, inducing them with RANKL and treating the cells with rBMP2 in the presence/absence of TWSG1 and CHRD. Osteoclasts will be quantified using TRAP staining and specific gene expression assessed via RT-qPCR.

From our second set of experiments, we observed that a loss of CHRD leads to osteoclast development. In addition, previous work by Graf et al., showed that CHRD was expressed in the damaged periodontium 5 days following ligature placement[51]. These observations warrant further investigation to explore the physiological effect of reduced CHRD expression on alveolar bone loss and subsequent recovery. One possible method to do this, involves placing ligatures on CHRD KO mice and control mice to induce inflammation and bone loss. These mice will be assessed with μCT (MILabs, Utrecht, Netherlands) prior to ligature placement, after alveolar bone loss, and following ligature removal to quantify bone loss/recovery and volume using Avizo software (Life Technologies). Subsequent investigations could then build on this by analyzing the long bones of CHRD KO mice for various bone parameters (trabecular thickness, trabecular spacing, trabecular volume) to assess the potential effect of lack of CHRD on bone mineral density.

Conclusion:

The periodontium can be viewed as having distinct components, all of which function together to maintain the integrity and protect the tooth complex. This harmony can also be found within the signalling pathways whether in response pathogens or mechanical response. It is this balance within the signalling network that ultimately controls bone remodelling. In this study we found that BMP2, TWSG1, and CHRD were dynamically expressed during osteoclast differentiation and that CHRD is not absolutely required for osteoclast formation. While this study plays a small part in highlighting the ways in which we can manipulate the signalling pathways, future studies should aim at finding all signalling pathways that regulate bone remodeling and their respective interconnections. Although previous studies have established the importance of M-CSF and RANKL in the formation of osteoclasts, the exact mechanisms involved in the phenotypic changes of precursor cells forming into active osteoclasts is not entirely known. Genome-wide identification of genes regulating osteoclastogenesis is the future of this field, and our study is one but a small piece of the puzzle that gives us the overall picture of the osteoclast differentiation process. Therefore, it is important to understand the signalling pathways involved in osteoclast formation and activation in order to benefit from new drug therapies for the prevention and treatment of bone loss.

References

1. Lang, N.P. and J. Lindhe, *Clinical periodontology and implant dentistry, 2 Volume Set*. 2015: John Wiley & Sons.
2. McKee, M., S. Zalzal, and A. Nanci, *Extracellular matrix in tooth cementum and mantle dentin: localization of osteopontin and other noncollagenous proteins, plasma proteins, and glycoconjugates by electron microscopy.* The Anatomical Record: An Official Publication of the American Association of Anatomists, 1996. **245**(2): p. 293-312.
3. Newman, M.G., et al., *Newman and Carranza's Clinical Periodontology for the Dental Hygienist-E-Book*. 2020: Elsevier Health Sciences.
4. Mcculloch, C.A., P. Lekic, and M.D. Mckee, *Role of physical forces in regulating the form and function of the periodontal ligament.* Periodontology 2000, 2000. **24**(1): p. 56-72.
5. Avery, J. and R. Rapp, *Pain conduction in human dental tissues.* Dent Clin North Am, 1959: p. 481-501.
6. Hasegawa, N., et al., *Immunohistochemical characteristics of epithelial cell rests of Malassez during cementum repair.* Journal of periodontal research, 2003. **38**(1): p. 51-56.
7. Saygin, N.E., W.V. Giannobile, and M.J. Somerman, *Molecular and cell biology of cementum.* Periodontology 2000, 2000. **24**(1): p. 73-98.
8. NP, L., *Bartold PM. Periodontal Health.* J Periodontol, 2018. **89**: p. s9-s16.
9. Brecx, M., et al., *Comparison between histological and clinical parameters during human experimental gingivitis.* Journal of periodontal research, 1987. **22**(1): p. 50-57.
10. Brecx, M., et al., *Variability of histologic criteria in clinically healthy human gingiva.* Journal of periodontal research, 1987. **22**(6): p. 468-472.
11. LINDHE, J. and H. RYLANDER, *Experimental gingivitis in young dogs.* European Journal of Oral Sciences, 1975. **83**(6): p. 314-326.
12. Canada, C.H., *Summary Report on the Findings of the Oral Health Component of the Canadian Health Measures Survey, 2007-2009*. 2010: Health Canada.
13. Pihlstrom, B.L., B.S. Michalowicz, and N.W. Johnson, *Periodontal diseases.* The lancet, 2005. **366**(9499): p. 1809-1820.
14. Page, R.C. and K.S. Kornman, *The pathogenesis of human periodontitis: an introduction.* Periodontology 2000, 1997. **14**(1): p. 9-11.
15. Crotti, T., et al., *Receptor activator NF κB ligand (RANKL) and osteoprotegerin (OPG) protein expression in periodontitis.* Journal of periodontal research, 2003. **38**(4): p. 380-387.
16. Liu, D., et al., *Expression of RANKL and OPG mRNA in periodontal disease: possible involvement in bone destruction.* International journal of molecular medicine, 2003. **11**(1): p. 17-21.
17. Buser, D., *20 years of Guided Bone Regeneration*. 2009: Quintessence Publishing.
18. Leder, B.Z. and M.N. Wein, *Osteoporosis: pathophysiology and clinical management*. 2020: Springer Nature.
19. Ducy, P., et al., *A Cbfa1-dependent genetic pathway controls bone formation beyond embryonic development.* Genes & development, 1999. **13**(8): p. 1025-1036.

20. Nakashima, K., et al., *The novel zinc finger-containing transcription factor osterix is required for osteoblast differentiation and bone formation.* Cell, 2002. **108**(1): p. 17-29.
21. Kenkre, J. and J. Bassett, *The bone remodelling cycle.* Annals of clinical biochemistry, 2018. **55**(3): p. 308-327.
22. Zhou, H., R. Chernecky, and J.E. Davies, *Deposition of cement at reversal lines in rat femoral bone.* Journal of bone and mineral research, 1994. **9**(3): p. 367-374.
23. Manolagas, S.C., *Birth and death of bone cells: basic regulatory mechanisms and implications for the pathogenesis and treatment of osteoporosis.* Endocrine reviews, 2000. **21**(2): p. 115-137.
24. for Bone, T.A.S., et al., *Proposed standard nomenclature for new tumor necrosis factor members involved in the regulation of bone resorption.* Bone, 2000. **27**(6): p. 761-764.
25. Kodama, H., et al., *Congenital osteoclast deficiency in osteopetrotic (op/op) mice is cured by injections of macrophage colony-stimulating factor.* The Journal of experimental medicine, 1991. **173**(1): p. 269-272.
26. Nakagawa, N., et al., *RANK is the essential signaling receptor for osteoclast differentiation factor in osteoclastogenesis.* Biochemical and biophysical research communications, 1998. **253**(2): p. 395-400.
27. Kong, Y.-Y., et al., *OPGL is a key regulator of osteoclastogenesis, lymphocyte development and lymph-node organogenesis.* Nature, 1999. **397**(6717): p. 315-323.
28. Li, J., et al., *RANK is the intrinsic hematopoietic cell surface receptor that controls osteoclastogenesis and regulation of bone mass and calcium metabolism.* Proceedings of the National Academy of Sciences, 2000. **97**(4): p. 1566-1571.
29. Hsu, H., et al., *Tumor necrosis factor receptor family member RANK mediates osteoclast differentiation and activation induced by osteoprotegerin ligand.* Proceedings of the National Academy of Sciences, 1999. **96**(7): p. 3540-3545.
30. Walsh, M.C. and Y. Choi, *Biology of the RANKL–RANK–OPG system in immunity, bone, and beyond.* Frontiers in immunology, 2014. **5**: p. 511.
31. Simonet, W., et al., *Osteoprotegerin: a novel secreted protein involved in the regulation of bone density.* Cell, 1997. **89**(2): p. 309-319.
32. Bucay, N., et al., *Osteoprotegerin-deficient mice develop early onset osteoporosis and arterial calcification.* Genes & development, 1998. **12**(9): p. 1260-1268.
33. Osta, B., *Effects of Interleukine-17A (Il-17A) and tumor necrosis factor alpha (TNF-α) on osteoblastic differentiation*. 2014, Université Claude Bernard-Lyon I.
34. Yagi, M., et al., *DC-STAMP is essential for cell–cell fusion in osteoclasts and foreign body giant cells.* The Journal of experimental medicine, 2005. **202**(3): p. 345-351.
35. Witwicka, H., et al., *Studies of OC-STAMP in osteoclast fusion: a new knockout mouse model, rescue of cell fusion, and transmembrane topology.* PLoS One, 2015. **10**(6): p. e0128275.
36. Lee, S.-H., et al., *v-ATPase V 0 subunit d2–deficient mice exhibit impaired osteoclast fusion and increased bone formation.* Nature medicine, 2006. **12**(12): p. 1403-1409.
37. Takayanagi, H., et al., *Induction and activation of the transcription factor NFATc1 (NFAT2) integrate RANKL signaling in terminal differentiation of osteoclasts.* Developmental cell, 2002. **3**(6): p. 889-901.

38. Asagiri, M. and H. Takayanagi, *The molecular understanding of osteoclast differentiation.* Bone, 2007. **40**(2): p. 251-264.
39. Novack, D.V. and R. Faccio, *Osteoclast motility: putting the brakes on bone resorption.* Ageing research reviews, 2011. **10**(1): p. 54-61.
40. Cappariello, A., et al., *The Great Beauty of the osteoclast.* Archives of biochemistry and biophysics, 2014. **558**: p. 70-78.
41. Zallone, A.Z., et al., *Osteoclasts and monocytes have similar cytoskeletal structures and adhesion property in vitro.* Journal of anatomy, 1983. **137**(Pt 1): p. 57.
42. Hunter, S.J., H. Schraer, and C.V. Gay, *Characterization of the cytoskeleton of isolated chick osteoclasts: effect of calcitonin.* Journal of Histochemistry & Cytochemistry, 1989. **37**(10): p. 1529-1537.
43. Georgess, D., et al., *Podosome organization drives osteoclast-mediated bone resorption.* Cell adhesion & migration, 2014. **8**(3): p. 192-204.
44. Wagner, D.O., et al., *BMPs: from bone to body morphogenetic proteins*. 2010, American Association for the Advancement of Science.
45. Lowery, J.W. and V. Rosen, *The BMP pathway and its inhibitors in the skeleton.* Physiological reviews, 2018. **98**(4): p. 2431-2452.
46. Westhrin, M., et al., *Bone morphogenetic protein 4 gene therapy in mice inhibits myeloma tumor growth, but has a negative impact on bone.* JBMR plus, 2020. **4**(1): p. e10247.
47. Jensen, E.D., et al., *Bone morphogenic protein 2 directly enhances differentiation of murine osteoclast precursors.* Journal of cellular biochemistry, 2010. **109**(4): p. 672-682.
48. Graf, D. and A.N. Economides, *Dissection of bone morphogenetic protein signaling using genome-engineering tools*, in *Bone morphogenetic proteins: from local to systemic therapeutics*. 2008, Springer. p. 115-139.
49. Sotillo Rodriguez, J.E., et al., *Enhanced osteoclastogenesis causes osteopenia in twisted gastrulation-deficient mice through increased BMP signaling.* Journal of Bone and Mineral Research, 2009. **24**(11): p. 1917-1926.
50. Pham, L., et al., *Bone morphogenetic protein 2 signaling in osteoclasts is negatively regulated by the BMP antagonist, twisted gastrulation.* Journal of cellular biochemistry, 2011. **112**(3): p. 793-803.
51. Graf, D., et al., *Common mechanisms in development and disease: BMP signaling in craniofacial development.* Cytokine & growth factor reviews, 2016. **27**: p. 129-139.
52. Carreira, A., et al., *Bone morphogenetic proteins: facts, challenges, and future perspectives.* Journal of dental research, 2014. **93**(4): p. 335-345.
53. Wei, F., et al., *The immunomodulatory role of BMP-2 on macrophages to accelerate osteogenesis.* Tissue Engineering Part A, 2018. **24**(7-8): p. 584-594.
54. Rakian, A., et al., *Bone morphogenetic protein-2 gene controls tooth root development in coordination with formation of the periodontium.* International journal of oral science, 2013. **5**(2): p. 75-84.
55. Ye, M., *Noggin-an antagonist of bone morphogenetic protein-is crucial for tooth hard tissue and periodontium development*. 2015, University of Zurich.
56. Wang, J., et al., *BMP1 and TLL1 are required for maintaining periodontal homeostasis.* Journal of dental research, 2017. **96**(5): p. 578-585.

57. Abe, T. and G. Hajishengallis, *Optimization of the ligature-induced periodontitis model in mice.* Journal of immunological methods, 2013. **394**(1-2): p. 49-54.
58. Kanatani, M., et al., *Stimulatory effect of bone morphogenetic protein-2 on osteoclast-like cell formation and bone-resorbing activity.* Journal of Bone and Mineral Research, 1995. **10**(11): p. 1681-1690.
59. Kaneko, H., et al., *Direct stimulation of osteoclastic bone resorption by bone morphogenetic protein (BMP)-2 and expression of BMP receptors in mature osteoclasts.* Bone, 2000. **27**(4): p. 479-486.
60. Onishi, T., et al., *Distinct and overlapping patterns of localization of bone morphogenetic protein (BMP) family members and a BMP type II receptor during fracture healing in rats.* Bone, 1998. **22**(6): p. 605-612.
61. Okamoto, M., et al., *Bone morphogenetic proteins in bone stimulate osteoclasts and osteoblasts during bone development.* Journal of Bone and Mineral Research, 2006. **21**(7): p. 1022-1033.
62. Canalis, E., A.N. Economides, and E. Gazzerro, *Bone morphogenetic proteins, their antagonists, and the skeleton.* Endocrine reviews, 2003. **24**(2): p. 218-235.
63. Larraín, J., et al., *BMP-binding modules in chordin: a model for signalling regulation in the extracellular space.* Development, 2000. **127**(4): p. 821-830.
64. Gazzerro, E., V. Gangji, and E. Canalis, *Bone morphogenetic proteins induce the expression of noggin, which limits their activity in cultured rat osteoblasts.* The Journal of clinical investigation, 1998. **102**(12): p. 2106-2114.
65. Graf, D., et al., *The developmentally regulated expression of Twisted gastrulation reveals a role for bone morphogenetic proteins in the control of T cell development.* The Journal of experimental medicine, 2002. **196**(2): p. 163-171.
66. Livak, K.J. and T.D. Schmittgen, *Analysis of relative gene expression data using real-time quantitative PCR and the 2− ΔΔCT method.* methods, 2001. **25**(4): p. 402-408.
67. Cappellen, D., et al., *Transcriptional program of mouse osteoclast differentiation governed by the macrophage colony-stimulating factor and the ligand for the receptor activator of NFκB.* Journal of Biological Chemistry, 2002. **277**(24): p. 21971-21982.
68. Tanaka, S., et al., *Macrophage colony-stimulating factor is indispensable for both proliferation and differentiation of osteoclast progenitors.* The Journal of clinical investigation, 1993. **91**(1): p. 257-263.
69. Arai, F., et al., *Commitment and differentiation of osteoclast precursor cells by the sequential expression of c-Fms and receptor activator of nuclear factor κB (RANK) receptors.* The Journal of experimental medicine, 1999. **190**(12): p. 1741-1754.
70. Lemma, S., et al., *Energy metabolism in osteoclast formation and activity.* The international journal of biochemistry & cell biology, 2016. **79**: p. 168-180.
71. Kim, J.-M., et al., *Osteoclast precursors display dynamic metabolic shifts toward accelerated glucose metabolism at an early stage of RANKL-stimulated osteoclast differentiation.* Cellular Physiology and Biochemistry, 2007. **20**(6): p. 935-946.
72. Boraschi-Diaz, I. and S.V. Komarova, *The protocol for the isolation and cryopreservation of osteoclast precursors from mouse bone marrow and spleen.* Cytotechnology, 2016. **68**(1): p. 105-114.

73. Takeshita, S., K. Kaji, and A. Kudo, *Identification and characterization of the new osteoclast progenitor with macrophage phenotypes being able to differentiate into mature osteoclasts.* Journal of Bone and Mineral Research, 2000. **15**(8): p. 1477-1488.
74. Oelgeschläger, M., et al., *The evolutionarily conserved BMP-binding protein Twisted gastrulation promotes BMP signalling.* Nature, 2000. **405**(6788): p. 757-763.
75. Piccolo, S., et al., *Cleavage of Chordin by Xolloid metalloprotease suggests a role for proteolytic processing in the regulation of Spemann organizer activity.* Cell, 1997. **91**(3): p. 407-416.
76. Rahman, M.M., et al., *Proliferation-coupled osteoclast differentiation by RANKL: Cell density as a determinant of osteoclast formation.* Bone, 2015. **81**: p. 392-399.

Appendix

In-vitro analysis of BMP2, CHRD, TWSG1 during osteoclast differentiation

Osteoclast Quantification

Multiple Comparisons

Dependent Variable: NumberofOsteoclast

	(I) Days	(J) Days	Mean Difference (I-J)	Std. Error	Sig.	95% Confidence Interval	
						Lower Bound	Upper Bound
Tukey HSD	Day 2	Day 4	-2.75000	7.00744	.979	-23.5544	18.0544
		Day 6	-71.25000*	7.00744	.000	-92.0544	-50.4456
		Day 8	-16.50000	7.00744	.140	-37.3044	4.3044
	Day 4	Day 2	2.75000	7.00744	.979	-18.0544	23.5544
		Day 6	-68.50000*	7.00744	.000	-89.3044	-47.6956
		Day 8	-13.75000	7.00744	.255	-34.5544	7.0544
	Day 6	Day 2	71.25000*	7.00744	.000	50.4456	92.0544
		Day 4	68.50000*	7.00744	.000	47.6956	89.3044
		Day 8	54.75000*	7.00744	.000	33.9456	75.5544
	Day 8	Day 2	16.50000	7.00744	.140	-4.3044	37.3044
		Day 4	13.75000	7.00744	.255	-7.0544	34.5544
		Day 6	-54.75000*	7.00744	.000	-75.5544	-33.9456

Gene expression

T-Test

Group Statistics

	Days	N	Mean	Std. Deviation	Std. Error Mean
BMP2Gene	Day 2 MCSF	4	1.0000	.00000	.00000
	Day 4 RANKL	4	9.1423	6.17555	3.08778

Independent Samples Test

		Levene's Test for Equality of Variances		t-test for Equality of Means						
		F	Sig.	t	df	Sig. (2-tailed)	Mean Difference	Std. Error Difference	95% Confidence Interval of the Difference	
									Lower	Upper
BMP2Gene	Equal variances assumed	7.427	.034	-2.637	6	.039	-8.14225	3.08778	-15.69777	-.58673
	Equal variances not assumed			-2.637	3.000	.078	-8.14225	3.08778	-17.96893	1.68443

T-Test

Group Statistics

	Days	N	Mean	Std. Deviation	Std. Error Mean
TWSG1Gene	Day 2 MCSF	4	1.0000	.00000	.00000
	Day 4 RANKL	4	5.1298	4.98363	2.49182

Independent Samples Test

		Levene's Test for Equality of Variances		t-test for Equality of Means						
									95% Confidence Interval of the Difference	
		F	Sig.	t	df	Sig. (2-tailed)	Mean Difference	Std. Error Difference	Lower	Upper
TWSG1Gene	Equal variances assumed	9.039	.024	-1.657	6	.149	-4.12975	2.49182	-10.22701	1.96751
	Equal variances not assumed			-1.657	3.000	.196	-4.12975	2.49182	-12.05982	3.80032

T-Test

Group Statistics

	Days	N	Mean	Std. Deviation	Std. Error Mean
CHRDGene	Day 2 MCSF	4	1.0000	.00000	.00000
	Day 4 RANKL	4	29.6428	46.96248	23.48124

Independent Samples Test

		Levene's Test for Equality of Variances		t-test for Equality of Means						
									95% Confidence Interval of the Difference	
		F	Sig.	t	df	Sig. (2-tailed)	Mean Difference	Std. Error Difference	Lower	Upper
CHRDGene	Equal variances assumed	8.875	.025	-1.220	6	.268	-28.64275	23.48124	-86.09928	28.81378
	Equal variances not assumed			-1.220	3.000	.310	-28.64275	23.48124	-103.37054	46.08504

T-Test

Group Statistics

	Days	N	Mean	Std. Deviation	Std. Error Mean
MMP9Gene	Day 2 MCSF	4	1.0000	.00000	.00000
	Day 4 RANKL	4	31909.3188	61127.7832	30563.8916

Independent Samples Test

		Levene's Test for Equality of Variances		t-test for Equality of Means						
									95% Confidence Interval of the Difference	
		F	Sig.	t	df	Sig. (2-tailed)	Mean Difference	Std. Error Difference	Lower	Upper
MMP9Gene	Equal variances assumed	8.999	.024	-1.044	6	.337	-31908.319	30563.8916	-106695.47	42878.8298
	Equal variances not assumed			-1.044	3.000	.373	-31908.319	30563.8916	-129176.26	65359.6251

T-Test

Group Statistics

	Days	N	Mean	Std. Deviation	Std. Error Mean
CTRGene	Day 2 MCSF	4	1.0000	.00000	.00000
	Day 4 RANKL	4	1571.5685	1632.64235	816.32117

Independent Samples Test

		Levene's Test for Equality of Variances		t-test for Equality of Means						
									95% Confidence Interval of the Difference	
		F	Sig.	t	df	Sig. (2-tailed)	Mean Difference	Std. Error Difference	Lower	Upper
CTRGene	Equal variances assumed	5.713	.054	-1.924	6	.103	-1570.5685	816.32117	-3568.0345	426.89746
	Equal variances not assumed			-1.924	3.000	.150	-1570.5685	816.32117	-4168.4668	1027.32981

T-Test

Group Statistics

	Days	N	Mean	Std. Deviation	Std. Error Mean
TRAPGene	Day 2 MCSF	4	1.0000	.00000	.00000
	Day 4 RANKL	4	706.1730	496.21801	248.10901

Independent Samples Test

		Levene's Test for Equality of Variances		t-test for Equality of Means						
									95% Confidence Interval of the Difference	
		F	Sig.	t	df	Sig. (2-tailed)	Mean Difference	Std. Error Difference	Lower	Upper
TRAPGene	Equal variances assumed	6.186	.047	-2.842	6	.029	-705.17300	248.10901	-1312.2739	-98.07213
	Equal variances not assumed			-2.842	3.000	.066	-705.17300	248.10901	-1494.7666	84.42059

T-Test

Group Statistics

	Days	N	Mean	Std. Deviation	Std. Error Mean
CTSKGene	Day 2 MCSF	4	1.0000	.00000	.00000
	Day 4 RANKL	4	263.3750	232.95197	116.47598

Independent Samples Test

		Levene's Test for Equality of Variances		t-test for Equality of Means						
									95% Confidence Interval of the Difference	
		F	Sig.	t	df	Sig. (2-tailed)	Mean Difference	Std. Error Difference	Lower	Upper
CTSKGene	Equal variances assumed	21.229	.004	-2.253	6	.065	-262.37500	116.47598	-547.38146	22.63146
	Equal variances not assumed			-2.253	3.000	.110	-262.37500	116.47598	-633.05356	108.30356

In-vitro analysis to determine whether CHRD directly controls osteoclast differentiation

Osteoclast Quantification

T-Test

Group Statistics

	Mousestrain	N	Mean	Std. Deviation	Std. Error Mean
NumberofOsteoclast	WT	3	38.3333	27.79089	16.04508
	CHRD KO	3	23.0000	19.51922	11.26943

Independent Samples Test

		Levene's Test for Equality of Variances		t-test for Equality of Means						
									95% Confidence Interval of the Difference	
		F	Sig.	t	df	Sig. (2-tailed)	Mean Difference	Std. Error Difference	Lower	Upper
NumberofOsteoclast	Equal variances assumed	.832	.413	.782	4	.478	15.33333	19.60725	-39.10513	69.77180
	Equal variances not assumed			.782	3.587	.483	15.33333	19.60725	-41.66825	72.33492

T-Test

Group Statistics

	Mousestrain	N	Mean	Std. Deviation	Std. Error Mean
NumberofOsteoclast	WT	3	18.0000	5.29150	3.05505
	CHRD KO	3	17.3333	7.23418	4.17665

Independent Samples Test

		Levene's Test for Equality of Variances		t-test for Equality of Means						
									95% Confidence Interval of the Difference	
		F	Sig.	t	df	Sig. (2-tailed)	Mean Difference	Std. Error Difference	Lower	Upper
NumberofOsteoclast	Equal variances assumed	.723	.443	.129	4	.904	.66667	5.17472	-13.70067	15.03401
	Equal variances not assumed			.129	3.664	.904	.66667	5.17472	-14.23579	15.56912

Gene expression

T-Test

Group Statistics

	Group	N	Mean	Std. Deviation	Std. Error Mean
MMP9	CHRDKO(LD)	3	171.3333	252.59520	145.83590
	WT(LD)	3	20.1000	24.86021	14.35305

Independent Samples Test

		Levene's Test for Equality of Variances		t-test for Equality of Means						
									95% Confidence Interval of the Difference	
		F	Sig.	t	df	Sig. (2-tailed)	Mean Difference	Std. Error Difference	Lower	Upper
MMP9	Equal variances assumed	12.901	.023	1.032	4	.360	151.23333	146.54051	-255.62835	558.09502
	Equal variances not assumed			1.032	2.039	.409	151.23333	146.54051	-467.93588	770.40255

T-Test

Group Statistics

	Group	N	Mean	Std. Deviation	Std. Error Mean
MMP9	CHRDKO(HD)	3	171.3333	252.59520	145.83590
	WT(HD)	3	20.1000	24.86021	14.35305

Independent Samples Test

		Levene's Test for Equality of		t-test for Equality of Means						
									95% Confidence Interval of the Difference	
		F	Sig.	t	df	Sig. (2-tailed)	Mean Difference	Std. Error Difference	Lower	Upper
MMP9	Equal variances assumed	12.901	.023	1.032	4	.360	151.23333	146.54051	-255.62835	558.09502
	Equal variances not assumed			1.032	2.039	.409	151.23333	146.54051	-467.93588	770.40255

Double-click to activate

T-Test

Group Statistics

	Group	N	Mean	Std. Deviation	Std. Error Mean
CTR	CHRDKO(LD)	3	9592.6667	15609.8382	9012.34430
	WT(LD)	3	17772.3333	30760.0690	17759.3341

Independent Samples Test

		Levene's Test for Equality of Variances		t-test for Equality of Means						
									95% Confidence Interval of the Difference	
		F	Sig.	t	df	Sig. (2-tailed)	Mean Difference	Std. Error Difference	Lower	Upper
CTR	Equal variances assumed	3.084	.154	-.411	4	.702	-8179.6667	19915.2278	-63473.203	47113.8700
	Equal variances not assumed			-.411	2.966	.709	-8179.6667	19915.2278	-71971.332	55611.9984

T-Test

Group Statistics

	Group	N	Mean	Std. Deviation	Std. Error Mean
CTR	CHRDKO(HD)	3	2326.0267	4022.66639	2322.48753
	WT(HD)	3	4599.5333	7965.23980	4598.73334

Independent Samples Test

		Levene's Test for Equality of Variances		t-test for Equality of Means						
									95% Confidence Interval of the Difference	
		F	Sig.	t	df	Sig. (2-tailed)	Mean Difference	Std. Error Difference	Lower	Upper
CTR	Equal variances assumed	3.123	.152	-.441	4	.682	-2273.5067	5151.92165	-16577.534	12030.5210
	Equal variances not assumed			-.441	2.958	.689	-2273.5067	5151.92165	-18802.037	14255.0234

T-Test

Group Statistics

	Group	N	Mean	Std. Deviation	Std. Error Mean
TRAP	CHRDKO(LD)	3	11273.6667	15876.7703	9166.45763
	WT(LD)	3	2595.0000	3381.76936	1952.46545

Independent Samples Test

		Levene's Test for Equality of Variances		t-test for Equality of Means						
									95% Confidence Interval of the Difference	
		F	Sig.	t	df	Sig. (2-tailed)	Mean Difference	Std. Error Difference	Lower	Upper
TRAP	Equal variances assumed	8.426	.044	.926	4	.407	8678.66667	9372.08978	-17342.426	34699.7595
	Equal variances not assumed			.926	2.181	.445	8678.66667	9372.08978	-28601.505	45958.8383

T-Test

Group Statistics

	Group	N	Mean	Std. Deviation	Std. Error Mean
TRAP	CHRDKO(HD)	3	129.3333	127.89579	73.84067
	WT(HD)	3	80.4333	90.12360	52.03288

Independent Samples Test

		Levene's Test for Equality of Variances		t-test for Equality of Means						
									95% Confidence Interval of the Difference	
		F	Sig.	t	df	Sig. (2-tailed)	Mean Difference	Std. Error Difference	Lower	Upper
TRAP	Equal variances assumed	.424	.551	.541	4	.617	48.90000	90.33197	-201.90177	299.70177
	Equal variances not assumed			.541	3.593	.620	48.90000	90.33197	-213.50195	311.30195

T-Test

Group Statistics

	Group	N	Mean	Std. Deviation	Std. Error Mean
CTSK	CHRDKO(LD)	3	357.0000	172.24401	99.44513
	WT(LD)	3	384.0000	342.21484	197.57783

Independent Samples Test

		Levene's Test for Equality of Variances		t-test for Equality of Means						
									95% Confidence Interval of the Difference	
		F	Sig.	t	df	Sig. (2-tailed)	Mean Difference	Std. Error Difference	Lower	Upper
CTSK	Equal variances assumed	.833	.413	-.122	4	.909	-27.00000	221.19298	-641.13016	587.13016
	Equal variances not assumed			-.122	2.952	.911	-27.00000	221.19298	-737.42422	683.42422

T-Test

Group Statistics

	Group	N	Mean	Std. Deviation	Std. Error Mean
CTSK	CHRDKO(HD)	3	1595.0000	2584.34653	1492.07317
	WT(HD)	3	257.7667	224.91568	129.85513

Independent Samples Test

		Levene's Test for Equality of Variances		t-test for Equality of Means						
									95% Confidence Interval of the Difference	
		F	Sig.	t	df	Sig. (2-tailed)	Mean Difference	Std. Error Difference	Lower	Upper
CTSK	Equal variances assumed	13.074	.022	.893	4	.422	1337.23333	1497.71315	-2821.0850	5495.55169
	Equal variances not assumed			.893	2.030	.465	1337.23333	1497.71315	-5015.6317	7690.09835